Stock assessment

2nd season 2018

Doryteuthis gahi

Andreas Winter

Natural Resources

Fisheries

December 2018

Index

Summary

1) The 2018 second season *Doryteuthis gahi* fishery (X license) was open from July 29th, and closed by directed order on September 30th. Compensatory days for mechanical problems and bad weather resulted in 38 vessel-days taken after September 30th, with two vessels fishing as late as October 4th.
2) Six fishing mortalities of Southern sea lions and thirteen fishing mortalities of South American fur seals were recorded throughout the course of the season. The use of Seal Exclusion Devices was mandated south of 52° S starting on August 5th, and mandated north of 52° S starting on August 7th.
3) 35,828 tonnes of *D. gahi* catch were reported in the X-license fishery; the highest 2nd season catch since 2010 and giving an average CPUE of 36.7 t vessel-day^{-1}. During the season 33.7% of *D. gahi* catch and 41.0% of fishing effort were taken north of 52º S; 66.3% of *D. gahi* catch and 59.0% of fishing effort were taken south of 52º S.
4) In the north sub-area, three depletion periods / immigrations were inferred to have started on July 29th (start of the season), August 31st, and September 30th. In the south sub-area, four depletion periods / immigrations were inferred to have started on July 29th, August 4th, August 10th, and August 30th.
5) A net emigration (negative immigration) was calculated for the season of 7,378 tonnes of *D. gahi* (95% confidence interval: –18,395 to 18,634 t), despite the occurrence of multiple in-season immigrations.
6) The escapement biomass estimate for *D. gahi* remaining in the Loligo Box at the end of second season 2018 was:
   Maximum likelihood of 35,910 tonnes, with a 95% confidence interval of 12,577 to 81,661 tonnes.
   The risk of *D. gahi* escapement biomass at the end of the season being less than 10,000 tonnes was estimated at 0.9%.

Introduction

The second season of the 2018 *Doryteuthis gahi* fishery (Patagonian longfin squid – colloquially *Loligo*) opened on July 29th with 16 X-licensed vessels. During the season 7 flex days were taken for mechanical repairs by various vessels, and one vessel required replacement shortly before the end. Thirty-six flex days were taken for bad weather, of which 6 on August 3rd, 10 on August 30th and 11 on September 4th (Figure 1). The season ended by directed closure on September 30th. The various schedule adjustments amounted to 38 vessel-days being taken after September 30th[a], with the last two vessels finishing on October 4th.

As in the previous season (Winter 2018), all X-license vessels were required to embark an observer tasked (at minimum) to monitor the presence and incidental capture of pinnipeds. The occurrence of pinniped mortalities resulted in mandatory use of Seal Exclusion Devices (SEDs) south of 52°S starting on August 5th, and north of 52°S starting on August 7th (that is to say everywhere in the fishery from August 7th).

Total reported *D. gahi* catch under second season X license was 35,828 tonnes (Table 1), the highest since 2010, and corresponding to an average CPUE of 35828 / 977 = 36.7 tonnes vessel-day^{-1}. Average CPUE was the highest on record in a second season (Table 1).

Assessment of the Falkland Islands *D. gahi* stock was conducted with depletion time-series models as in previous seasons (Agnew et al. 1998, Roa-Ureta and Arkhipkin 2007;

[a] One vessel with a partial season allocation expended its flex days earlier than September 30th.

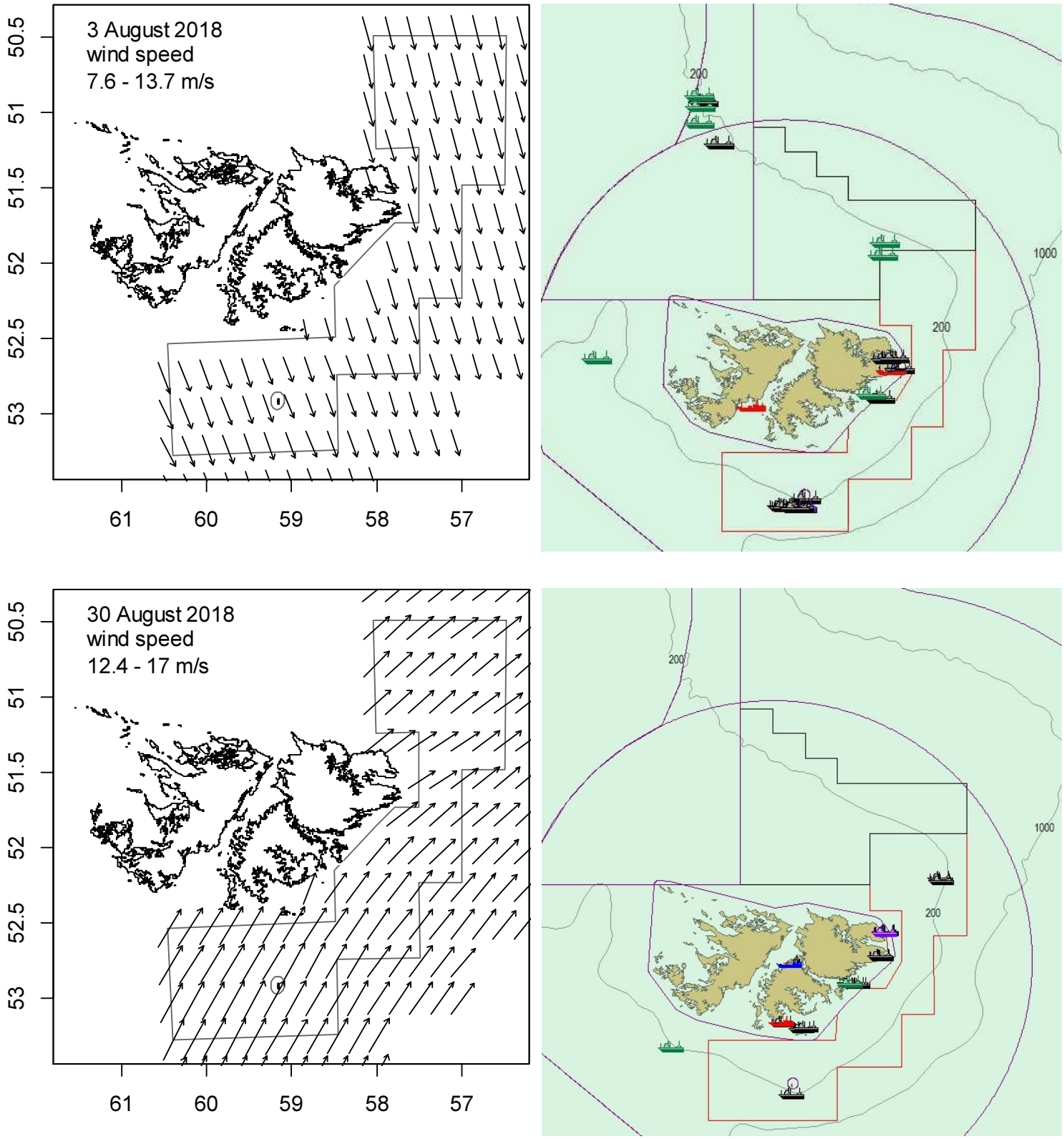

Figure 1. Left: wind speed vector plot at 0.25° resolution, from blended satellite observations (Zhang et al., 2006). Right: Fish Ops chart display. Top: August 3rd, when 6 X-licensed vessels declared bad-weather days, bottom: August 30th, when 10 X-licensed vessels declared bad-weather days.

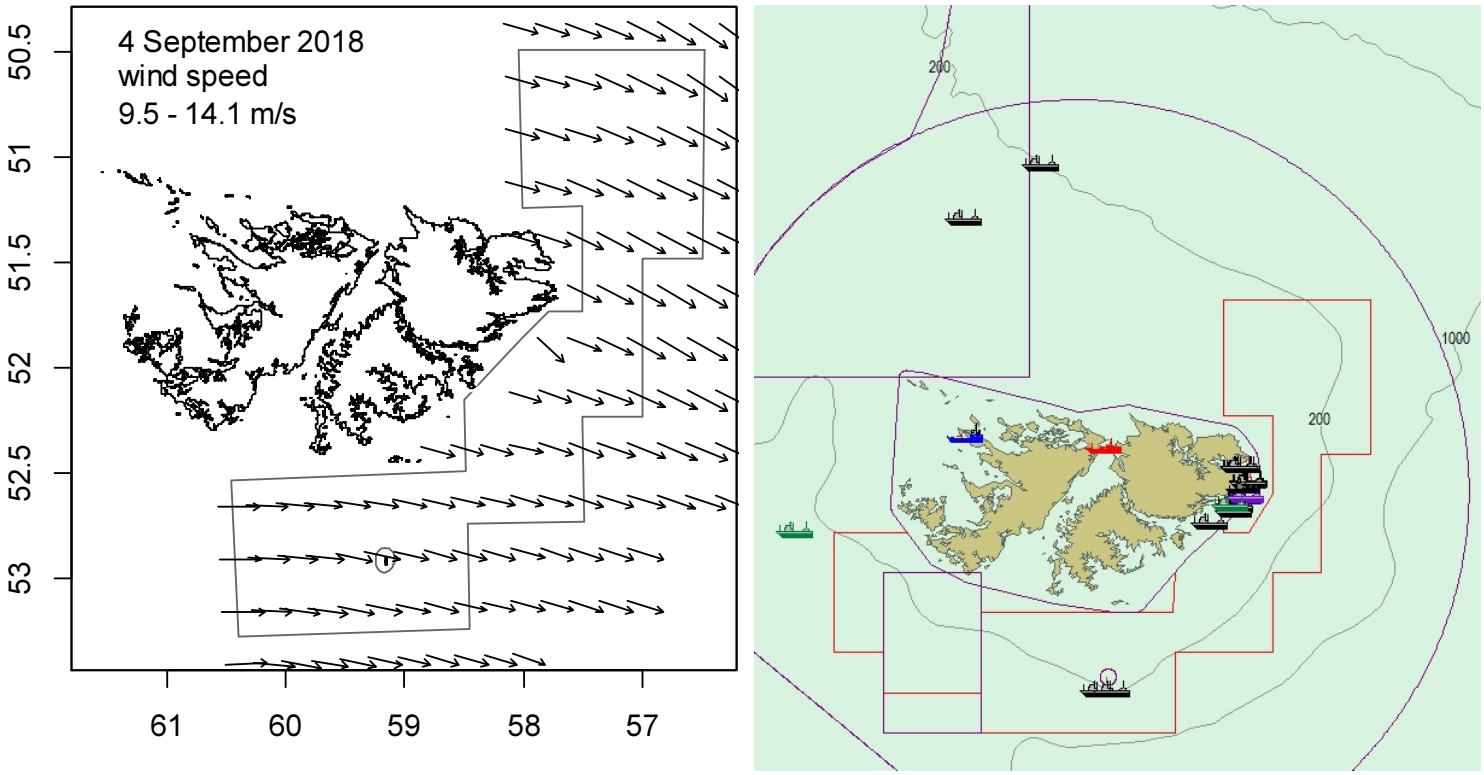

Figure 1 (concluded). September 4th, when 11 X-licensed vessels declared bad-weather days.

Arkhipkin et al. 2008), and in other squid fisheries (Royer et al. 2002, Young et al. 2004, Chen et al. 2008, Morales-Bojórquez et al. 2008, Keller et al. 2015, Medellín-Ortiz et al. 2016). Because *D. gahi* has an annual life cycle (Patterson 1988, Arkhipkin 1993), stock cannot be derived from a standing biomass carried over from prior years (Rosenberg et al. 1990, Pierce and Guerra 1994). The depletion model instead calculates an estimate of population abundance over time by evaluating what levels of abundance and catchability must be extant to sustain the observed rate of catch. Depletion modelling of the *D. gahi* target fishery is used both in-season and for the post-season summary, with the objective of maintaining an escapement biomass of 10,000 tonnes *D. gahi* at the end of each season as a conservation threshold (Agnew et al. 2002, Barton 2002).

Methods

The depletion model formulated for the Falklands *D. gahi* stock is based on the equivalence:

$$C_{day} = q \times E_{day} \times N_{day} \times e^{-M/2} \quad \textbf{(1)}$$

where q is the catchability coefficient, M is the natural mortality rate (considered constant at 0.0133 day^{-1}; Roa-Ureta and Arkhipkin 2007), and C_{day}, E_{day}, N_{day} are catch (numbers of squid), fishing effort (numbers of vessels), and abundance (numbers of squid) per day. In its basic form (DeLury 1947) the depletion model assumes a closed population in a fixed area for the duration of the assessment. However, the assumption of a closed population is

imperfectly met in the Falkland Islands fishery, where stock analyses have often shown that *D. gahi* groups arrive in successive waves after the start of the season (Roa-Ureta 2012; Winter and Arkhipkin 2015). Arrivals of successive groups are inferred from discontinuities in the catch data. Fishing on a single, closed cohort would be expected to yield gradually decreasing CPUE, but gradually increasing average individual sizes, as the squid grow. When instead these data change suddenly, or in contrast to expectation, the immigration of a new group to the population is indicated (Winter and Arkhipkin 2015).

Table 1. *D. gahi* season comparisons since 2004, when catch management was assumed by the FIFD. Days: total number of calendar days open to licensed *D. gahi* fishing including (since 1st season 2013) optional extension days; V-Days: aggregate number of licensed *D. gahi* fishing days reported by all vessels for the season. Entries in italics are seasons closed by emergency order.

	Season 1			Season 2		
	Catch (t)	Days	V-Days	Catch (t)	Days	V-Days
2004	7,152	46	625	17,559	78	1271
2005	24,605	45	576	29,659	78	1210
2006	19,056	50	704	*23,238*	*53*	*883*
2007	17,229	50	680	*24,171*	*63*	*1063*
2008	24,752	51	780	26,996	78	1189
2009	12,764	50	773	*17,836*	*59*	*923*
2010	28,754	50	765	36,993	78	1169
2011	15,271	50	771	*18,725*	*70*	*1099*
2012	34,767	51	770	35,026	78	1095
2013	19,908	53	782	19,614	78	1195
2014	28,119	59	872	19,630	71	1099
2015	*19,383**	*57**	*871**	*10,190*	*42*	*665*
2016	22,616	68	1020	23,089	68	1004
2017	39,433	68	999†	24,101	69	1002‡
2018	43,085	69	975	35,828	68	977

* Does not include C-license catch or effort after the C-license target for that season was switched from *D. gahi* to *Illex*.
† Includes two vessel-days of experimental fishing for juvenile toothfish.
‡ Includes one vessel-day of experimental fishing for juvenile toothfish.

In the event of a new group arrival, the depletion calculation must be modified to account for this influx. This is done using a simultaneous algorithm that adds new arrivals on top of the stock previously present, and posits a common catchability coefficient for the entire depletion time-series. If two depletions are included in the same model (i.e., the stock present from the start plus a new group arrival), then:

$$C_{day} = q \times E_{day} \times (N1_{day} + (N2_{day} \times i2|_0^1)) \times e^{-M/2} \quad \textbf{(2)}$$

where i2 is a dummy variable taking the values 0 or 1 if 'day' is before or after the start day of the second depletion. For more than two depletions, $N3_{day}$, i3, $N4_{day}$, i4, etc., would be included following the same pattern.

Because SEDs were mandated in this season, the SED modification of the depletion model developed last year (Winter 2017b) was implemented again for the stock assessment:

$$C_{day} = q_{SED} \times E_{SED\text{-}day} \times (N1_{day} + (N2_{day} \times i2|_0^1)) \times e^{-M/2} + q_{NSED} \times E_{NSED\text{-}day} \times (N1_{day} + (N2_{day} \times i2|_0^1)) \times e^{-M/2} \quad \textbf{(3)}$$

whereby the depletion catch Equation **2** is formulated as the composite of fishing effort in parallel with and without SEDs (subscripts SED and NSED). As before, the computational difference between q_{SED} and q_{NSED} includes not only the technical efficacy of either gear but all fishing aspects that correlate with the gear; e.g., that vessels fishing under SED 'conditions' might stop a trawl when pinnipeds are sighted, or switch locations more frequently or distantly.

The season depletion likelihood function was calculated as the difference between actual catch numbers reported and catch numbers predicted from the model (Equation **3**), statistically corrected by a factor relating to the number of days of the depletion period (Roa-Ureta 2012):

$$((n\text{Days} - 2)/2) \times \log\left(\sum_{days}\left(\log(\text{predicted}\,C_{day}) - \log(\text{actual}\,C_{day})\right)^2\right) \quad \textbf{(4)}$$

The stock assessment was set in a Bayesian framework (Punt and Hilborn 1997), whereby results of the season depletion model are conditioned by prior information on the stock; in this case the information from the pre-season survey.

The likelihood function of prior information was calculated as the normal distribution of the difference between catchability (q) derived from the survey abundance estimate, and catchability derived from the season depletion model. Applying this difference requires both the survey and the season to be fishing the same stock with the same gear. Catchability, rather than abundance N, is used for calculating prior likelihood because catchability informs the entire season time series; whereas N from the survey only informs the first in-season depletion period – subsequent immigrations and depletions are independent of the abundance that was present during the survey. In this season, only NSED fishing was conducted in the pre-season survey (Winter et al. 2018), and therefore only q_{NSED} could be linked to a prior. Thus, the prior likelihood function was:

$$\frac{1}{\sqrt{2\pi \cdot SD_{q\,prior\,NSED}^{\,2}}} \times \exp\left(-\frac{(q_{model\,NSED} - q_{prior\,NSED})^2}{2 \cdot SD_{q\,prior\,NSED}^{\,2}}\right) \quad \textbf{(5)}$$

where the standard deviation of catchability prior ($SD_{q\ prior\ NSED}$) was calculated from the Euclidean sum of the survey prior estimate uncertainty, the variability in catches on the season start date, and the uncertainty in the natural mortality M estimate over the number of days mortality discounting (Appendix: Equations **A5-N**, **A5-S**).

Bayesian optimization of the depletion was calculated by jointly minimizing Equations **4** and **5**, using the Nelder-Mead algorithm in R programming package 'optimx' (Nash and Varadhan 2011). Relative weights in the joint optimization were assigned to Equations **4** and **5** as the converse of their coefficients of variation (CV), i.e., the CV of the prior became the weight of the depletion model and the CV of the depletion model became the weight of the prior. Calculations of the CVs are described in Equations **A8-N** and **A8-S**. Because a complex model with multiple depletions may converge on a local minimum rather than global minimum, the optimization was stabilized by running a feed-back loop that set the q and N parameter outputs of the Bayesian joint optimization back into the in-season-only

minimization (Equation **4**), re-calculated this minimization and the CV resulting from it, then re-calculated the Bayesian joint optimization, and continued this process until both the in-season minimization and the joint optimization remained unchanged.

With actual C_{day}, $E_{NSED\text{ - }day}$, $E_{SED\text{ - }day}$, and M being fixed parameters, the optimization of Equation **3** using **4** and **5** produces estimates of q_{NSED}, q_{SED}, and N1, N2, …, etc. Numbers of squid on the final day (or any other day) of a time series are then calculated as the numbers N of the depletion start days discounted for natural mortality during the intervening period, and subtracting cumulative catch also discounted for natural mortality (CNMD). Taking for example a two-depletion period:

$$\begin{aligned} N_{final\ day} &= N1_{start\ day\ 1} \times e^{-M\ (final\ day\ -\ start\ day\ 1)} \\ &+ N2_{start\ day\ 2} \times e^{-M\ (final\ day\ -\ start\ day\ 2)} \\ &- CNMD_{final\ day} \end{aligned} \quad \textbf{(6)}$$

where

$$CNMD_{day\ 1} = 0$$

$$CNMD_{day\ x} = CNMD_{day\ x-1} \times e^{-M} + C_{day\ x-1} \times e^{-M/2} \quad \textbf{(7)}$$

$N_{final\ day}$ is then multiplied by the average individual weight of squid on the final day to give biomass. Daily average individual weight is obtained from length / weight conversion of mantle lengths measured in-season by observers, and also derived from in-season commercial data as the proportion of product weight that vessels reported per market size category. Observer mantle lengths are scientifically accurate, but restricted to 1-2 vessels at any one time that may or may not be representative of the entire fleet, and not available every day. Commercially proportioned mantle lengths are relatively less accurate, but cover the entire fishing fleet every day. Therefore, both sources of data are used (see Appendix – *Doryteuthis gahi* individual weights).

Distributions of the likelihood estimates from joint optimization (i.e., measures of their statistical uncertainty) were computed using a Markov Chain Monte Carlo (MCMC) (Gamerman and Lopes 2006), a method that is commonly employed for fisheries assessments (Magnusson et al. 2013). MCMC is an iterative process which generates random stepwise changes to the proposed outcome of a model (in this case, the q and N of *D. gahi* squid) and at each step, accepts or nullifies the change with a probability equivalent to how well the change fits the model parameters compared to the previous step. The resulting sequence of accepted or nullified changes (i.e., the 'chain') approximates the likelihood distribution of the model outcome. The MCMC of the depletion models were run for 200,000 iterations; the first 1000 iterations were discarded as burn-in sections (initial phases over which the algorithm stabilizes); and the chains were thinned by a factor equivalent to the maximum of either 5 or the inverse of the acceptance rate (e.g., if the acceptance rate was 12.5%, then every 8^{th} (0.125^{-1}) iteration was retained) to reduce serial correlation. For each model three chains were run; one chain initiated with the parameter values obtained from the joint optimization of Equations **4** and **5**, one chain initiated with these parameters ×2, and one chain initiated with these parameters ×¼. Convergence of the three chains was accepted if the variance among chains was less than 10% higher than the variance within chains (Brooks and Gelman 1998). When convergence was satisfied the three chains were combined as one final set. Equations **6**, **7**, and the multiplication by average individual weight were applied to the CNMD and each iteration of N values in the final set, and the biomass outcomes from these calculations represent the distribution of the estimate. The peaks of the MCMC histograms were compared to the empirical optimizations of the N values.

Depletion models and likelihood distributions were calculated separately for north and south sub-areas of the Loligo Box fishing zone, as *D. gahi* sub-stocks emigrate from different spawning grounds and remain to an extent segregated (Arkhipkin and Middleton 2002). Total escapement biomass is then defined as the aggregate biomass of *D. gahi* on the last day of the season for north and south sub-areas combined. North and south biomasses are not assumed to be uncorrelated however (Shaw et al. 2004), and therefore north and south likelihood distributions were added semi-randomly in proportion to the strength of their day-to-day correlation (see Winter 2014, for the semi-randomization algorithm).

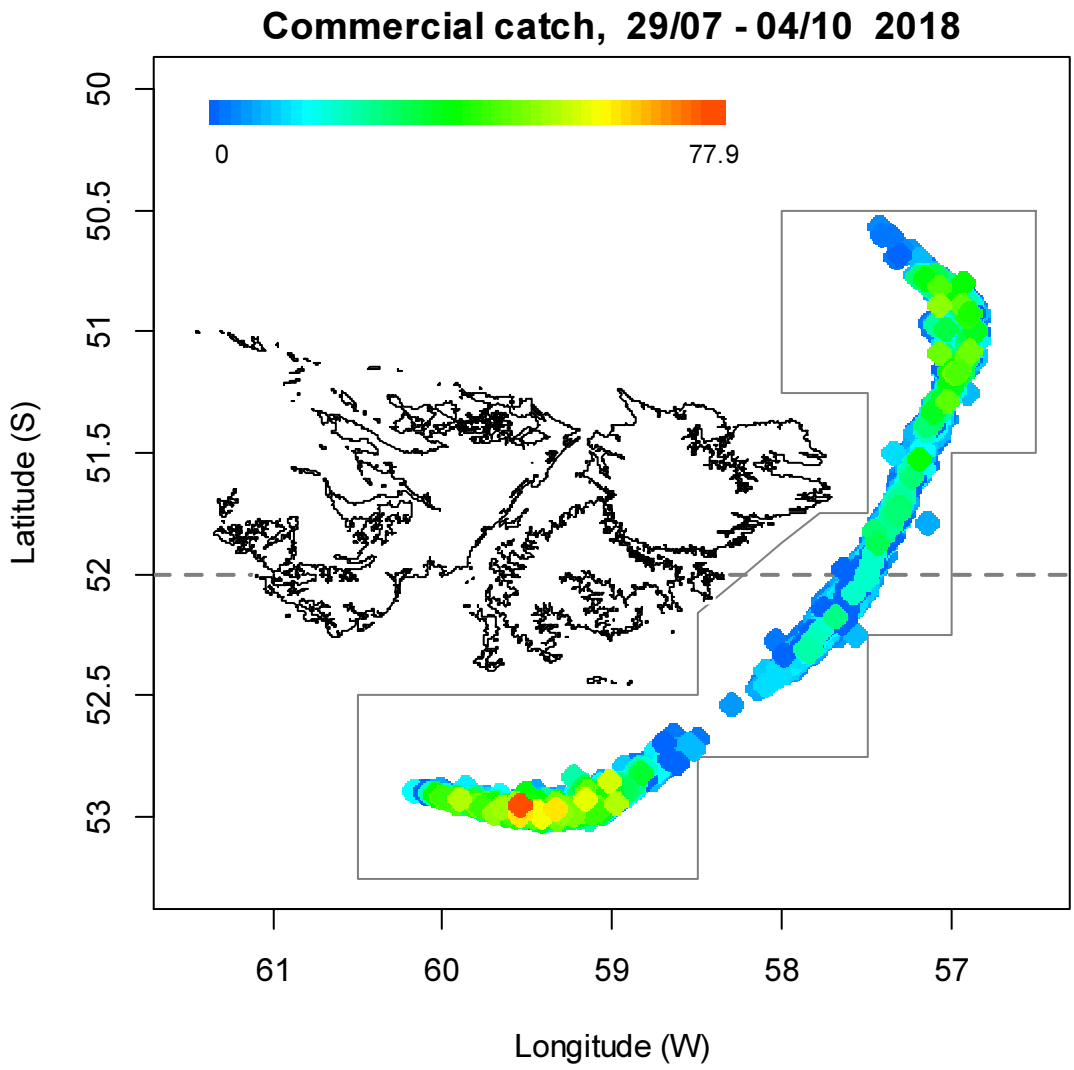

Figure 2. Spatial distribution of *D. gahi* 2nd-season trawls, colour-scaled to catch weight (max. = 77.9 tonnes). 3263 trawls were taken during the season. The 'Loligo Box' fishing zone, as well as the 52 ºS parallel delineating the boundary between north and south assessment sub-areas, are shown in grey.

Stock assessment
Data

With no in-season area closures for the first time since 1st season 2017, *D. gahi* catch and effort (Figure 2) were relatively balanced north and south: 33.7% of catch (12068 t) and

41.0% of effort (400.1 vessel-days) were taken north of 52°S, 66.3% of catch (23760 t) and 59.0% of effort (576.9) were taken south of 52°S. In the south, more than 67% of catch was taken in the first 3 weeks of the 68-day season (Figure 3). In the north, catches were more even but still preponderant with 67% taken in the first half of the season (Figure 3).

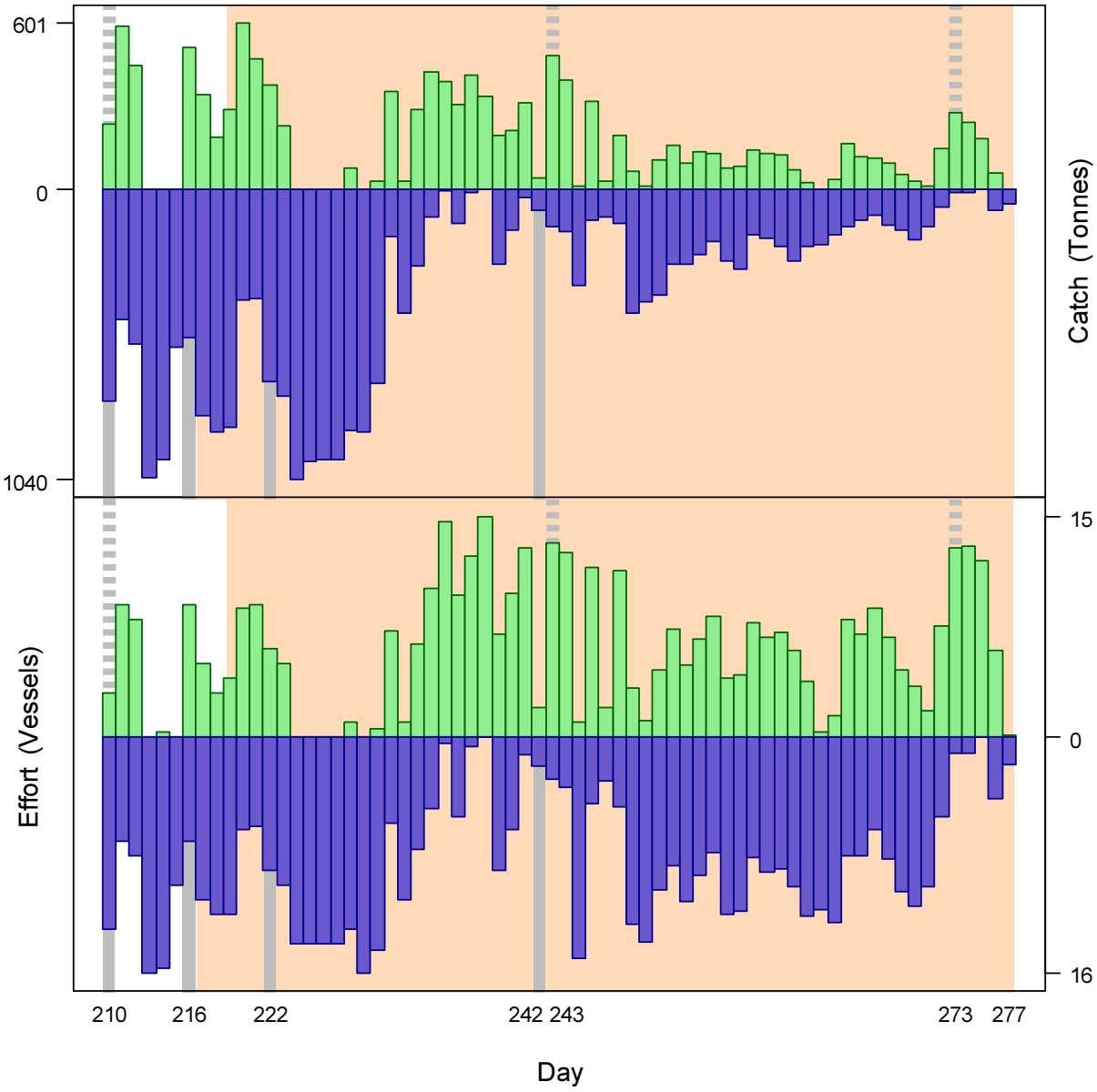

Figure 3. Daily total *D. gahi* catch and effort distribution by assessment sub-area north (green) and south (purple) of latitude 52° S during 2nd season 2018. The season was open from July 29th (chronological day 210) to September 30th (chronological day 273), plus flex days until October 4th (day 277). Orange under-shading delineates the mandatory use of SEDs north and south. As many as 15 vessels fished per day north; as many as 16 vessels fished per day south. As much as 601 tonnes *D. gahi* was caught per day north; as much as 1040 tonnes *D. gahi* was caught per day south.

977 vessel-days were fished during the season (Table 1), with a median of 15 vessels per day (mean 14.7) except for flex and weather extensions. Vessels reported daily catch totals to the FIFD and electronic logbook data that included trawl times, positions, depths,

and product weight by market size categories. Three FIG fishery observers were deployed in the fishing season for a total of 48 sampling days[b] (Thomas 2018, Chemshirova 2018a, b, Trevizan 2018). Throughout the 68 days of the season, 25 days had no FIG fishery observer covering (including 2 of the 4 season-end extension days), 38 days had 1 FIG fishery observer covering, and 5 days had two FIG fishery observers covering. Except for seabird days FIG fishery observers were tasked with sampling 200 *D. gahi* at two stations; reporting their maturity stages, sex, and lengths to 0.5 cm. Contract marine mammal monitors were tasked with measuring 200 unsexed lengths of *D. gahi* per day. The length-weight relationship for converting observer and commercially proportioned lengths was combined from 2nd pre-season and season data of both 2017 and 2018, as 2018 data became available progressively. The final parameterization of the length-weight relationship included 5995 measures from 2017 and 1417 measures from 2018, giving:

$$\text{weight (kg)} = 0.16578 \times \text{length (cm)}^{2.20549} / 1000 \quad \textbf{(8)}$$

with a coefficient of determination $R^2 = 94.8\%$.

Group arrivals / depletion criteria

Start days of depletions - following arrivals of new *D. gahi* groups - were judged primarily by daily changes in CPUE, with additional information from sex proportions, maturity, and average individual squid sizes. CPUE was calculated as metric tonnes of *D. gahi* caught per vessel per day. Days were used rather than trawl hours as the basic unit of effort. Commercial vessels do not trawl standardized duration hours, but rather durations that best suit their daily processing requirements. An effort index of days is therefore more consistent.

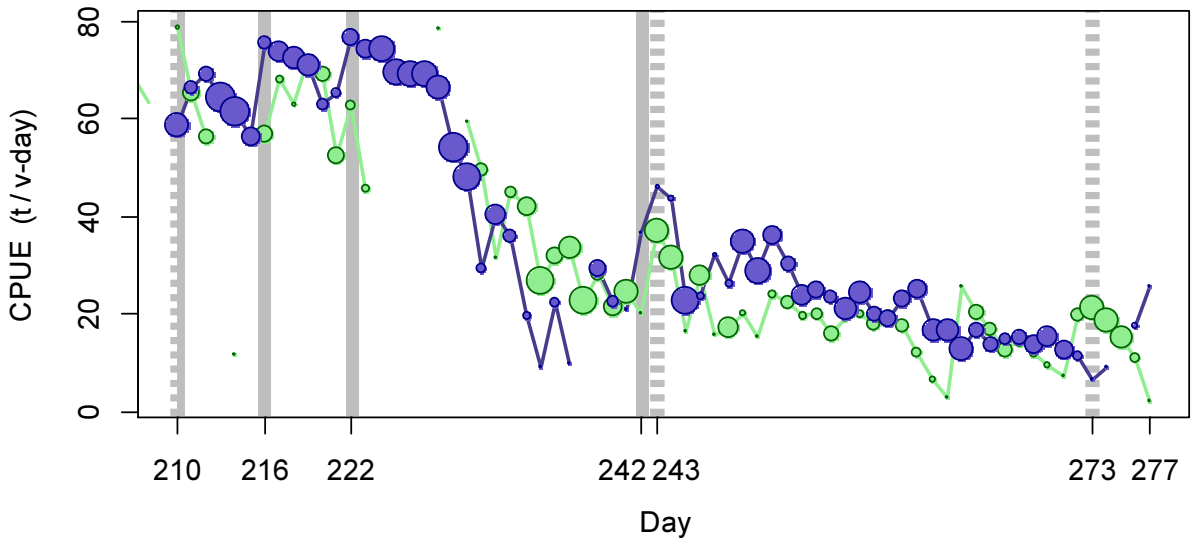

Figure 4. CPUE in metric tonnes per vessel per day, by assessment sub-area north (green) and south (purple) of 52° S latitude. Circle sizes are proportioned to numbers of vessels fishing. Data from consecutive days are joined by line segments. Broken grey bars indicate the starts of in-season depletions north. Solid grey bars indicate the starts of in-season depletions south.

[b] Not counting seabird days (every fourth day).

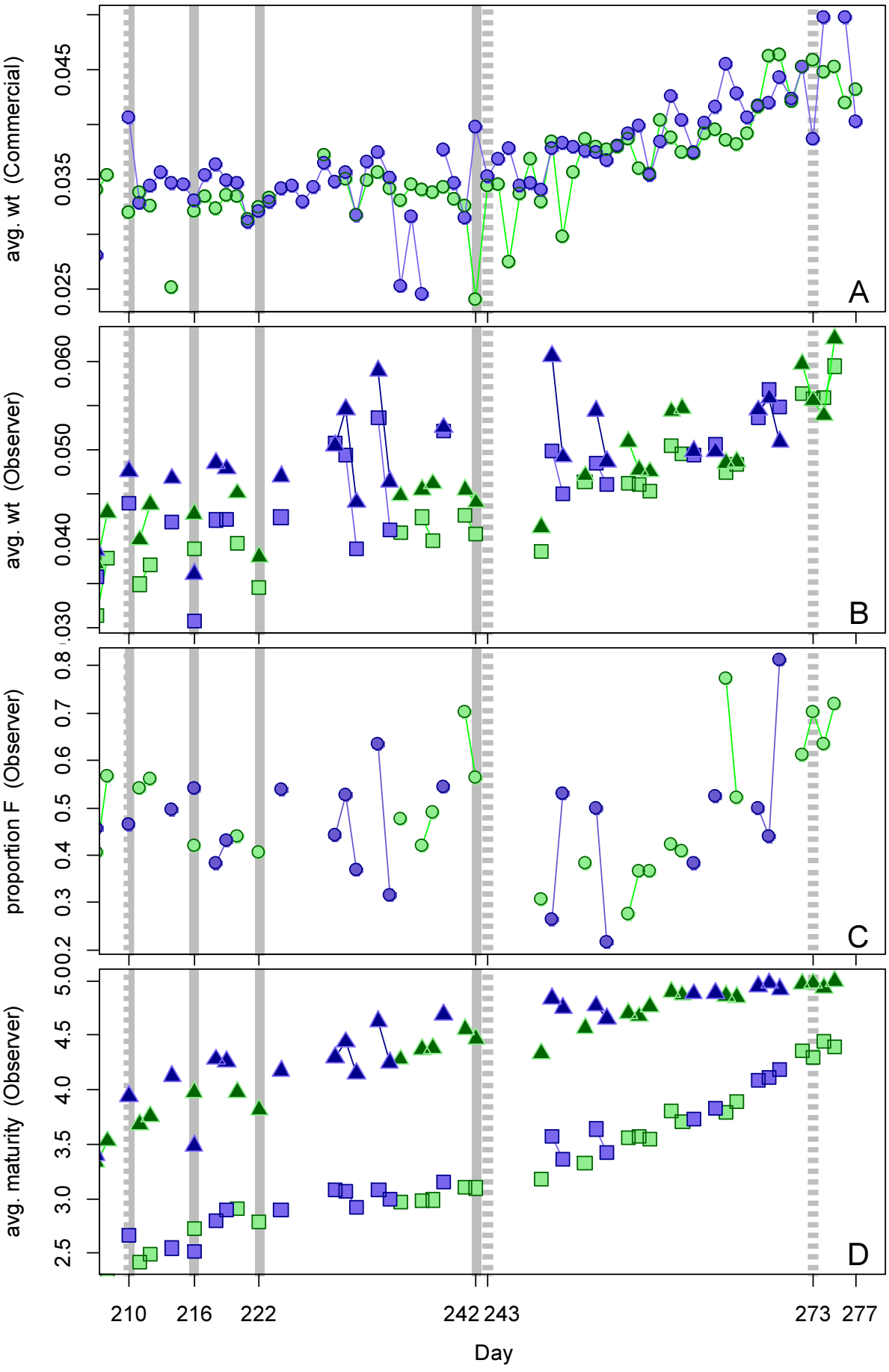
avg. wt (Commercial)
0.025
0.035
0.045
A
avg. wt (Observer)
0.030
0.040
0.050
0.060
B
proportion F (Observer)
0.2
0.3
0.4
0.5
0.6
0.7
0.8
C
avg. maturity (Observer)
2.5
3.0
3.5
4.0
4.5
5.0
D
210
216
222
242
243
273
277
Day

Figure 5 [previous page]. A: Average individual *D. gahi* weights (kg) per day from commercial size categories. B: Average individual *D. gahi* weights (kg) by sex per day from observer sampling. C: Proportions of female *D. gahi* per day from observer sampling. D: Average maturity value by sex per day from observer sampling. In all graphs – Males: triangles, females: squares, unsexed: circles. North sub-area: green, south sub-area: purple. Data from consecutive days are joined by line segments. Broken grey bars indicate the starts of in-season depletions north. Solid grey bars indicate the starts of in-season depletions south.

Three days in the north and four days in the south were identified that represented the onset of separate immigrations / depletions throughout the season. An interesting pattern showed that all in-season immigrations in the south occurred before any of the in-season immigrations in the north.

- The first depletion north was set on day 210 (July 29th), the first day of fishing in the north sub-area (by three vessels). CPUE was highest for the season (Figure 4); average observer weight and maturity were close to the lowest of the season (Figure 5B and D).
- The second depletion north was identified on day 243 (August 31st) with a pronounced increase in CPUE (Figure 4), the day after the season low average commercial weight and an apparent local peak in female proportion (Figure 5A and C).
- The third depletion north was identified on day 273 (September 30th; the last scheduled day of the season) with the highest CPUE by at least two vessels in 3 weeks (Figure 4) and a local minimum in average observer weight (Figure 5B).
- The first depletion south was set on day 210 (July 29th), the first day of fishing in the south sub-area (by thirteen vessels). Average maturity was approximately the low starting point of the season, while average commercial weight appeared anomalously high, but dropped the next day to a lower level consistent with the season trend (Figure 5D and A).
- The second depletion south was identified on day 216 (August 4th), with a sharp increase in CPUE (Figure 4) and local dips in average commercial weight, average observer weight, and average maturity (Figure 5A, B, and D).
- The third depletion south was identified on day 222 (August 10th) when CPUE took another increase, to its highest level of the season (Figure 4), the day after the lowest average commercial weight of the season up to that point (Figure 5A).
- The fourth depletion south was set on day 242 (August 30th) when CPUE increased following a decreasing trend over 16 days (Figure 4).

Depletion analyses
North

In the north sub-area, Bayesian optimization was weighted at 0.594 for in-season depletion (**A5-N**) vs. 0.317 for the prior (**A8-N**). Bayesian optimization on catchability (q) without SEDs resulted in a maximum likelihood posterior of ${}_{\text{Bayesian}}q_{\text{N NSED}} = 1.635 \times 10^{-3}$ (Figure 6, left, and Equation **A9-N**). The pre-season prior was slightly lower at ${}_{\text{prior}}q_{\text{N}} = 1.325 \times 10^{-3}$; Figure 6, left, and Equation **A4-N**), while in-season depletion optimized much higher at ${}_{\text{depletion}}q_{\text{N NSED}} = 2.741 \times 10^{-3}$ (off the scale on Figure 6, left, and **A6-N**). With only a short period of fishing before SEDs were mandated, the in-season ${}_{\text{depletion}}q_{\text{N NSED}}$ had a predictably weak effect on the model, despite its higher weighting.

Posterior catchability with SEDs was substantially higher at ${}_{\text{Bayesian}}q_{\text{N SED}} = 2.937 \times 10^{-3}$ (Equation **A9-N**). As in both previous seasons (Winter 2017b, Winter 2018), this implies

that fishing with a SED in the net had higher squid catch efficacy than fishing without a SED, and as in both previous seasons, the outcome is difficult to separate from collinear factors. A Wilcoxon rank-sum test found that in the north, the catch rate of *D. gahi* in kg per hour was marginally higher (p = 0.053) two days after the switch to SEDs (August 7th and 8th) than two days before the switch to SEDs (August 5th and 6th).

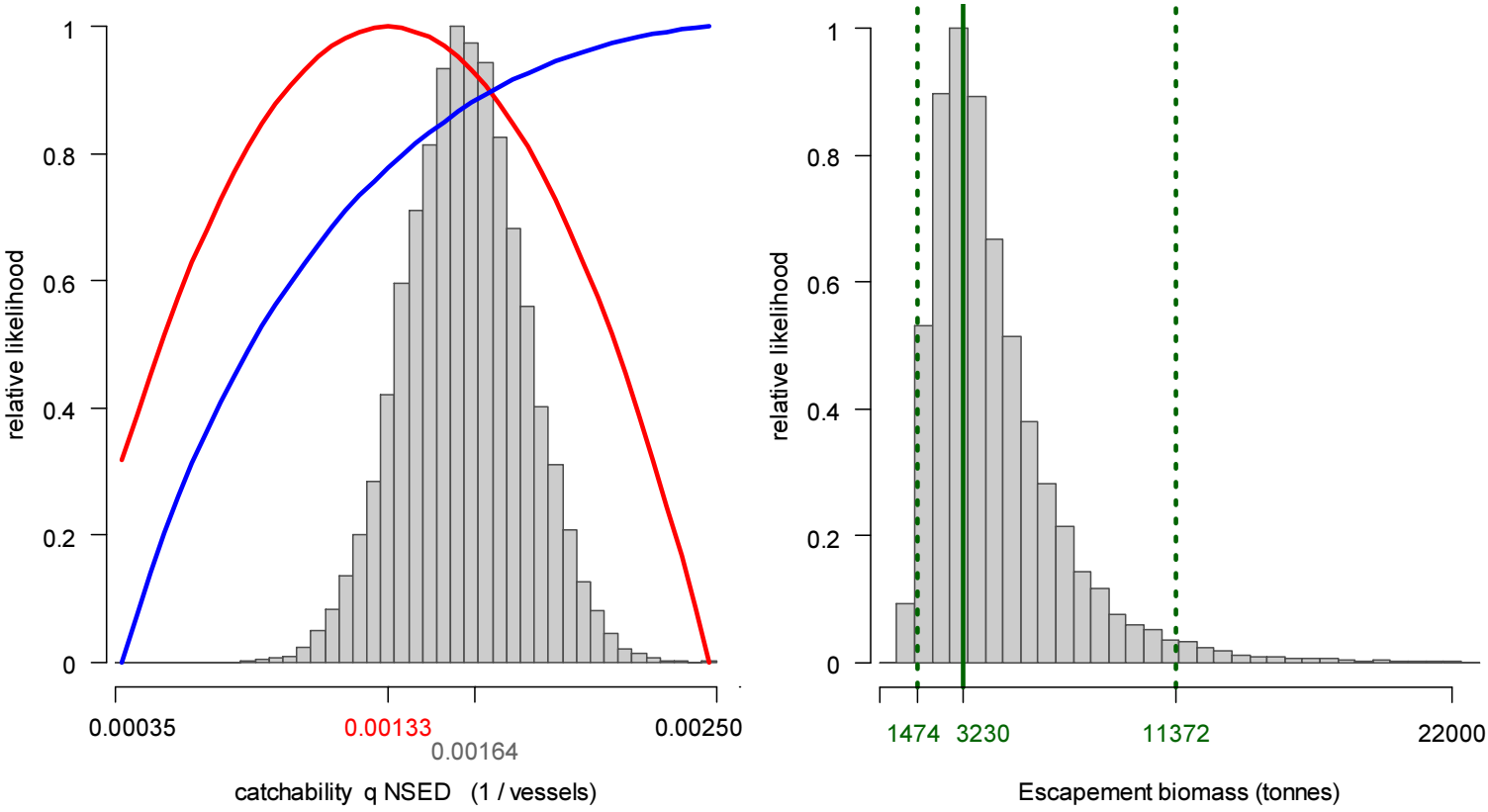

Figure 6. North sub-area. Left: Likelihood distributions for *D. gahi* NSED catchability. Red line: prior model (pre-season survey data), blue line: in-season depletion model, grey bars: combined Bayesian model posterior. Right: Likelihood distribution (grey bars) of escapement biomass, from Bayesian posterior and average individual squid weight at the end of the season. Green lines: maximum likelihood and 95% confidence interval. Note the correspondence to Figure 7.

The MCMC distribution of the Bayesian posterior multiplied by the generalized additive model (GAM) fit of average individual squid weight (Figure A1-north) gave the likelihood distribution of *D. gahi* biomass on day 277 (October 4th) shown in Figure 6-right, with maximum likelihood and 95% confidence interval of:

$$B_{N\ day\ 277} = 3{,}230\ t \sim 95\%\ CI\ [1{,}474 - 11{,}372]\ t \quad \textbf{(9)}$$

At its highest point (the start of the season: day 210 – July 29th), model-estimated *D. gahi* biomass north was 22,648 t ~ 95% CI [19,423 – 37,602] t (Figure 7). This biomass estimate at the start of the season was significantly lower than the pre-season survey estimate (Winter et al. 2018). The survey estimate may have been biased high as in much of the area, no bound was identified on the spatial extent of high densities.

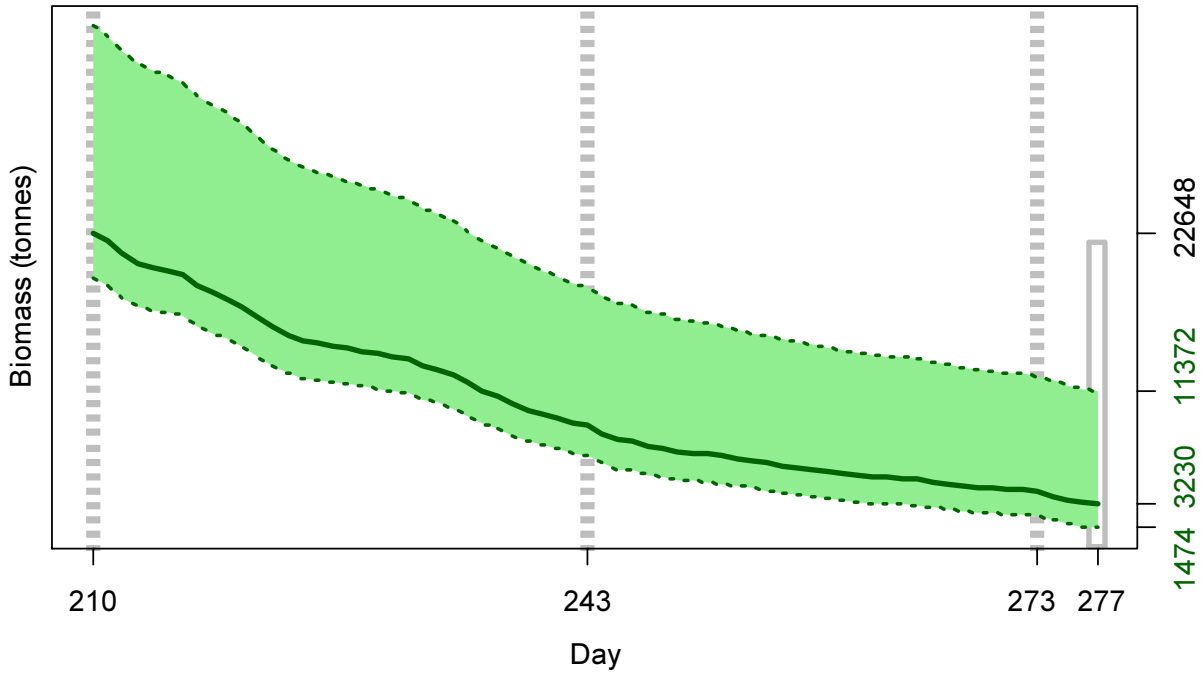

Figure 7. North sub-area. *D. gahi* biomass time series estimated from Bayesian posterior of the depletion model ± 95% confidence intervals. Broken grey bars indicate the start of in-season depletions north; days 210, 243, and 273. Note that the biomass 'footprint' on day 277 (October 4th) corresponds to the right-side plot of Figure 6.

South

In the south sub-area, Bayesian optimization was weighted nearly equally at 0.555 for in-season depletion (**A5-S**) vs. 0.538 for the prior (**A8-S**). Bayesian optimization on catchability q without SEDs resulted in a maximum likelihood posterior ($_{\text{Bayesian}}\, q_{\text{S NSED}} = 0.544 \times 10^{-3}$; Figure 8, left, and Equation **A9-S**) that was slightly higher than the pre-season prior ($_{\text{prior}}\, q_{\text{S}} = 0.498 \times 10^{-3}$; Figure 8, left, and Equation **A4-S**). In-season depletion was higher than the maximum of the MCMC distribution at $_{\text{depletion}}\, q_{\text{S NSED}} = 1.681 \times 10^{-3}$ (off the scale on Figure 8, left, and **A6-S**). As in the north, the short N SED fishing period early in the season resulted in a weak effect of $_{\text{depletion}}\, q_{\text{S NSED}}$, and the early part of the season was characterized by poor fit of the depletion model (Figure A2-S).

Posterior catchability with SEDs was $_{\text{Bayesian}}\, q_{\text{S SED}} = 0.575 \times 10^{-3}$ (Equation **A9-S**), thus only moderately higher than $_{\text{Bayesian}}\, q_{\text{S NSED}}$. A Wilcoxon rank-sum test found that in the south, *D. gahi* kg per hour was significantly higher ($p = 0.0024$) two days after the switch to SEDs (August 5th and 6th) than two days before the switch to SEDs (August 3rd and 4th). The significant result is unsurprising as an immigration occurred on August 4th (Figure 4); just before SEDs were mandated, and the relatively small difference between $_{\text{Bayesian}}\, q_{\text{S NSED}}$ and $_{\text{Bayesian}}\, q_{\text{S NSED}}$ suggests that an SED has less effect on catch rates when abundance is high.

Figure 8 [below]. South sub-area. Left: Likelihood distributions for *D. gahi* NSED catchability. Red line: prior model (pre-season survey data), blue line: in-season depletion model, grey bars: combined Bayesian model posterior. Right: Likelihood distribution (grey bars) of escapement biomass, from Bayesian posterior and average individual squid weight at the end of the season. Blue lines: maximum likelihood and 95% confidence interval. Note correspondence to Figure 9.

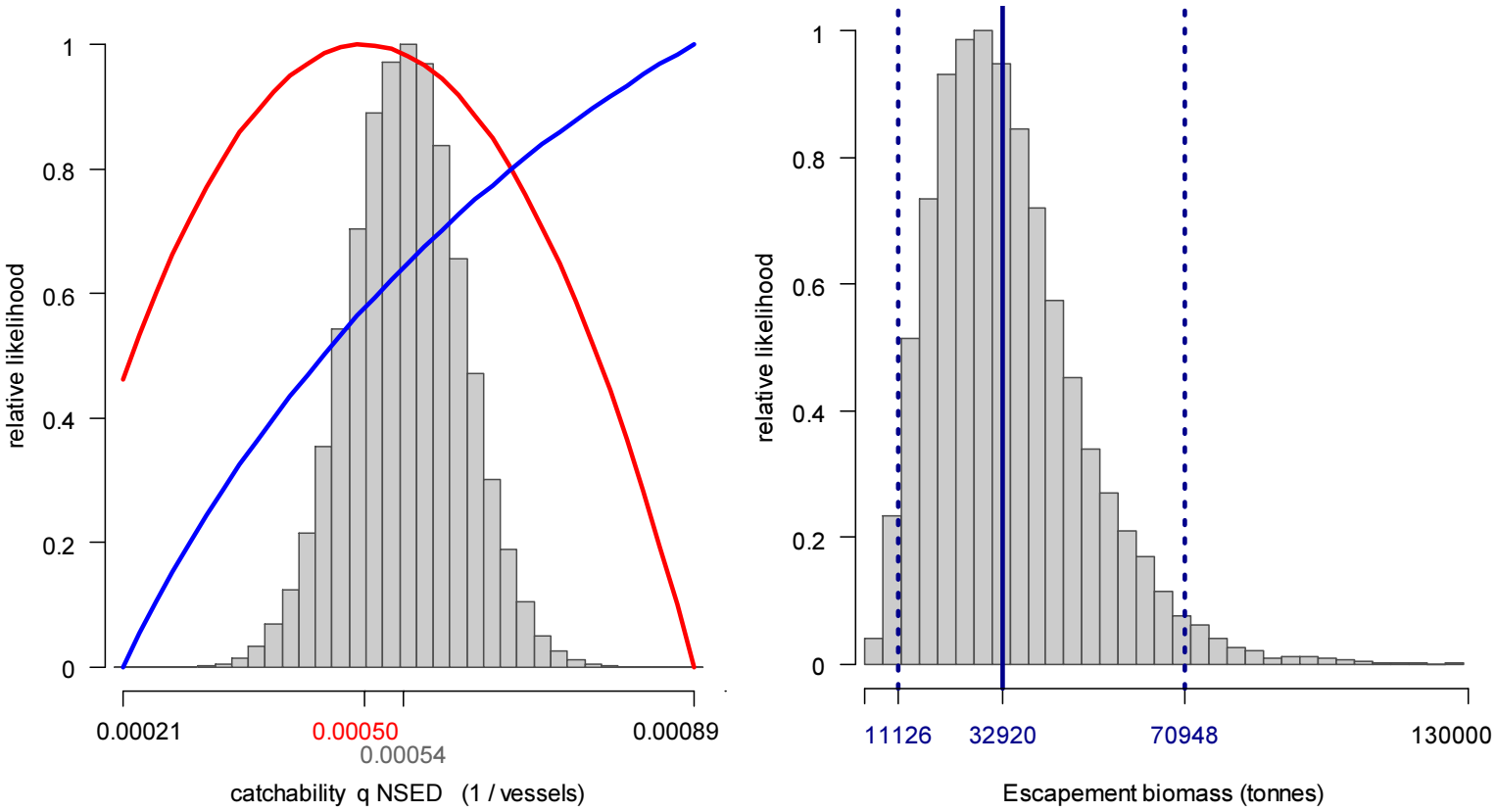

Figure 9 [below]. South sub-area. *D. gahi* biomass time series estimated from Bayesian posterior of the depletion model ± 95% confidence intervals. Grey bars indicate the start of in-season depletions south; days 210, 216, 222, and 242. Note that the biomass 'footprint' on day 277 (October 4th) corresponds to the right-side plot of Figure 8.

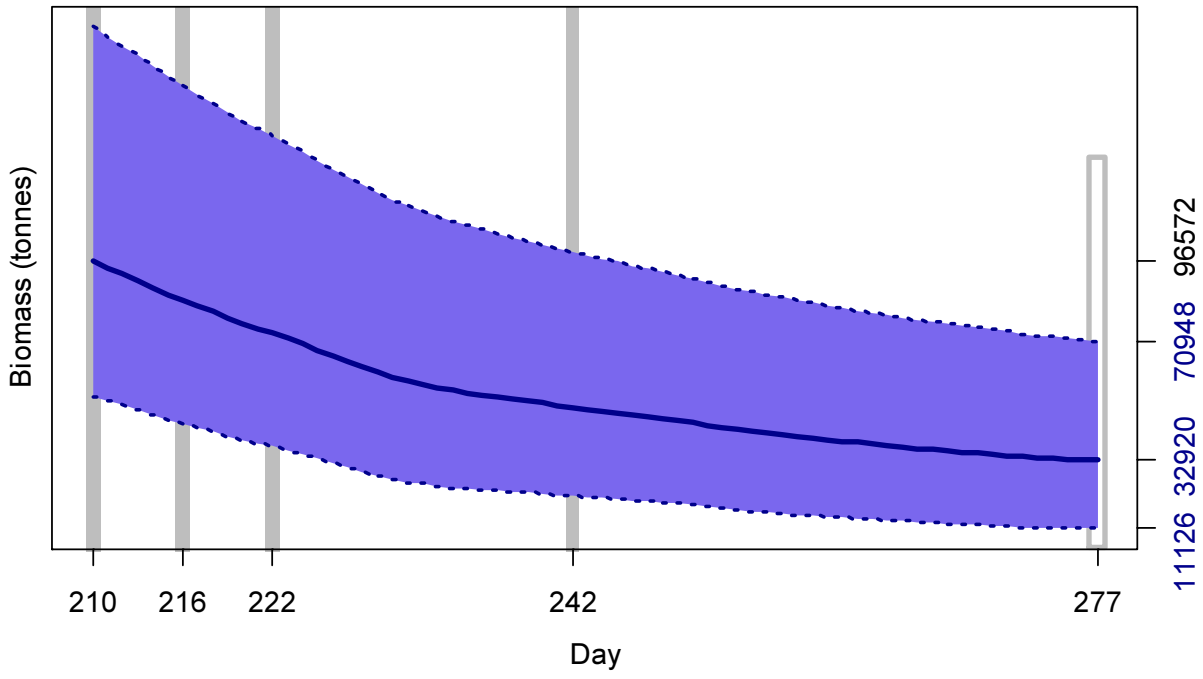

The MCMC distribution of the Bayesian posterior multiplied by the GAM fit of average individual squid weight (Figure A1-south) gave the likelihood distribution of *D. gahi* biomass on day 277 (October 4th) shown in Figure 8-right, with maximum likelihood and 95% confidence interval of:

$$B_{S\ day\ 277} = 32{,}920\ t \sim 95\%\ CI\ [11{,}126 – 70{,}948]\ t \quad \textbf{(10)}$$

At its highest point (the start of the season: day 210 – July 29th), estimated *D. gahi* biomass south was 96,572 t ~ 95% CI [53,515 – 171,701] t (Figure 9). This was lower but unlike the north, not significantly different from the pre-season survey estimate (Winter et al. 2018). Variability remained high throughout the time period, and it is not statistically conclusive that any change in average biomass occurred during the season by the rule that a straight line could be drawn through the plot (Figure 9) without intersecting the 95% confidence intervals (Swartzman et al. 1992).

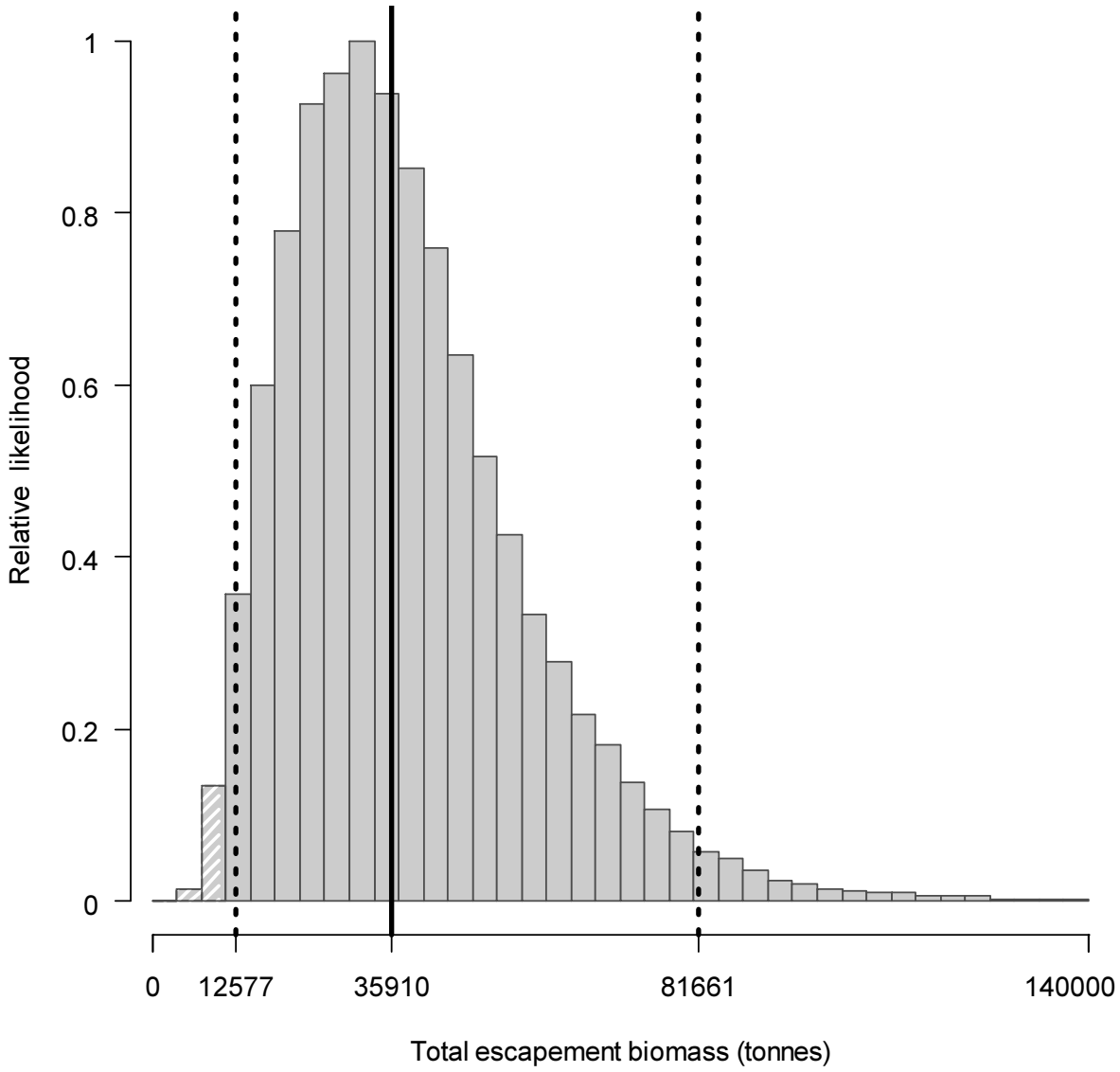

Figure 10 [previous page]. Likelihood distribution with 95% confidence intervals of total *D. gahi* escapement biomass at the season end (October 4th). White shading lines; portion of the distribution < 10,000 tonnes; equal to 0.9% of the whole distribution.

Escapement biomass

Total escapement biomass was defined as the aggregate biomass of *D. gahi* at the end of day 277 (October 4th) for north and south sub-areas combined (Equations **9** and **10**). Depletion models are calculated on the inference that all fishing and natural mortality are gathered at mid-day, thus a half day of mortality ($e^{-M/2}$) was added to correspond to the closure of the fishery at 23:59:59 (mid-night) on October 4th for the final remaining vessels: Equation **11**. Semi-randomized addition of the north and south biomass estimates gave the aggregate likelihood distribution of total escapement biomass shown in Figure 10.

$$B_{\text{Total day 277}} = (B_{\text{N day 277}} + B_{\text{S day 277}}) \times e^{-M/2}$$

$$= 36{,}150 \text{ t} \times 0.99336$$

$$= 35{,}910 \text{ t} \sim 95\% \text{ CI } [12{,}577 - 81{,}661] \text{ t} \quad \textbf{(11)}$$

The estimated escapement biomass of 35,910 t was the highest for a second season since at least 2005. The risk of the fishery in the current season, defined as the proportion of the total escapement biomass distribution below the conservation limit of 10,000 tonnes (Agnew et al., 2002; Barton, 2002), was calculated as 0.9%.

Immigration

Doryteuthis gahi immigration during the season was inferred on each day by how many more squid were estimated present than the day before, minus the number caught and the number expected to have died naturally:

$$_{\text{Immigration}}N_{\text{day i}} = N_{\text{day i}} - (N_{\text{day i-1}} - C_{\text{day i-1}} - M_{\text{day i-1}})$$

where $N_{\text{day i-1}}$ are optimized in the depletion models, $C_{\text{day i-1}}$ calculated as in Equation **3**, and $M_{\text{day i-1}}$ is:

$$M_{\text{day i-1}} = (N_{\text{day i-1}} - C_{\text{day i-1}}) \times (1 - e^{-M})$$

Immigration biomass per day was then calculated as the immigration number per day multiplied by predicted average individual weight from the GAM:

$$_{\text{Immigration}}B_{\text{day i}} = {}_{\text{Immigration}}N_{\text{day i}} \times {}_{\text{GAM}}Wt_{\text{day i}}$$

All numbers N are themselves derived from the daily average individual weights, therefore the estimation automatically factors in that those squid immigrating on a given day would likely be smaller than average (because younger). Confidence intervals of the immigration estimates were calculated by applying the above algorithms to the MCMC iterations of the

depletion models. Resulting total biomasses of *D. gahi* immigration north and south, up to season end (day 277), were:

$$_{\text{Immigration}}B_{\text{N season}} = -2{,}051 \text{ t} \sim 95\% \text{ CI } [-3{,}407 \text{ to } -308] \text{ t} \quad \textbf{(12-N)}$$

$$_{\text{Immigration}}B_{\text{S season}} = -5{,}327 \text{ t} \sim 95\% \text{ CI } [-15{,}247 \text{ to } 18{,}680] \text{ t} \quad \textbf{(12-S)}$$

Total immigration with semi-randomized addition of the confidence intervals was:

$$_{\text{Immigration}}B_{\text{Total season}} = -7{,}378 \text{ t} \sim 95\% \text{ CI } [-18{,}634 \text{ to } +18{,}395] \text{ t} \quad \textbf{(12-T)}$$

The calculations indicate that net emigration occurred during the season, albeit with high uncertainty, especially in the south. Although a typical number of immigration events were identified (Figures 4 and 5), these had visibly little impact on the biomass time series during the season (Figures 7 and 9) and evidently did not outweigh the numbers of squid present from the start and escaping both capture and natural mortality to move into deeper water. While unusual compared to other recent seasons, a balance of net emigration is plausible given the exceptionally high biomass at the start of the season (Winter et al. 2018).

Pinniped bycatch

Pinniped bycatch during 2nd season 2018 totalled 19 reported fishing mortalities; 13 South American fur seals (*Arctocephalus australis*) and 6 Southern sea lions (*Otaria flavescens*), distributed as summarized in Table 2 and Figure 11. The distribution of pinniped fishing mortalities was analysed for correlation with SEDs, aggregation by trawl and by vessel, daylight[c], position (latitude / longitude), trawl duration, and sea state. Correlations were tested by randomly re-distributing 100000× the pinniped mortalities among the 3263 commercial trawls during the season and calculating the proportions of the 100000 iterations that exceeded the empirical parameters[d]. The non-overlap between South American fur seal and Southern sea lion mortalities (Table 2) was also tested by these randomized re-distributions. All tests except non-overlap were calculated separately for the two pinniped species. Because the analysis implied multiple comparisons among stochastically independent null hypotheses, significance thresholds were adjusted by the Šidák correction:

$$\alpha_{\text{corr}} = 1 - (1 - \alpha)^{\frac{1}{m}} = 1 - (1 - 0.05)^{\frac{1}{5}} = 0.0102 \quad \textbf{(13)}$$

where α = the standard significance threshold of p = 0.05, and m = number of independent null hypotheses: SED, daylight, position, duration, sea state; thus m = five[e]. The analysis was restricted to mortalities as live captures are ambiguous to quantify: escapees cannot be counted accurately and the same animals may be caught repeatedly (especially if they're habituated, therefore non-independence of counts).

[c] Daylight is defined as a trawl hauled between sunrise and sunset, calculated using the algorithms of the NOAA Earth System research laboratory, www.esrl.noaa.gov/gmd/grad/solcalc/calcdetails.html.
[d] Either counts or weighted means.
[e] Latitude and longitude, although computed separately, were considered part of the same position parameter, therefore only one null hypothesis including both. Aggregation of trawls and vessels were tested but unlike the other parameters are not causative agents of mortality, therefore not part of the same 'family' of null hypotheses. As vessels are nested within trawls there was also no separate 2-fold significance correction for trawl and vessel aggregation.

Table 2. Reported fishing mortalities of pinnipeds, by trawl, in 2nd season 2018.

Date	Species	No.	Grid at haul
Aug 1st	South American fur seal	1	XVAK
Aug 3rd	South American fur seal	3	XVAJ
Aug 6th	Southern sea lion	4	XNAQ
Sep 1st	South American fur seal	1	XVAK
Sep 3rd	South American fur seal	1	XVAK
Sep 5th	South American fur seal	1	XVAJ
Sep 6th	South American fur seal	1	XVAK
Sep 8th	South American fur seal	3	XVAK
Sep 9th	Southern sea lion	2	XVAK
Sep 11th	South American fur seal	1	XVAK
Sep 23rd	South American fur seal	1	XVAL

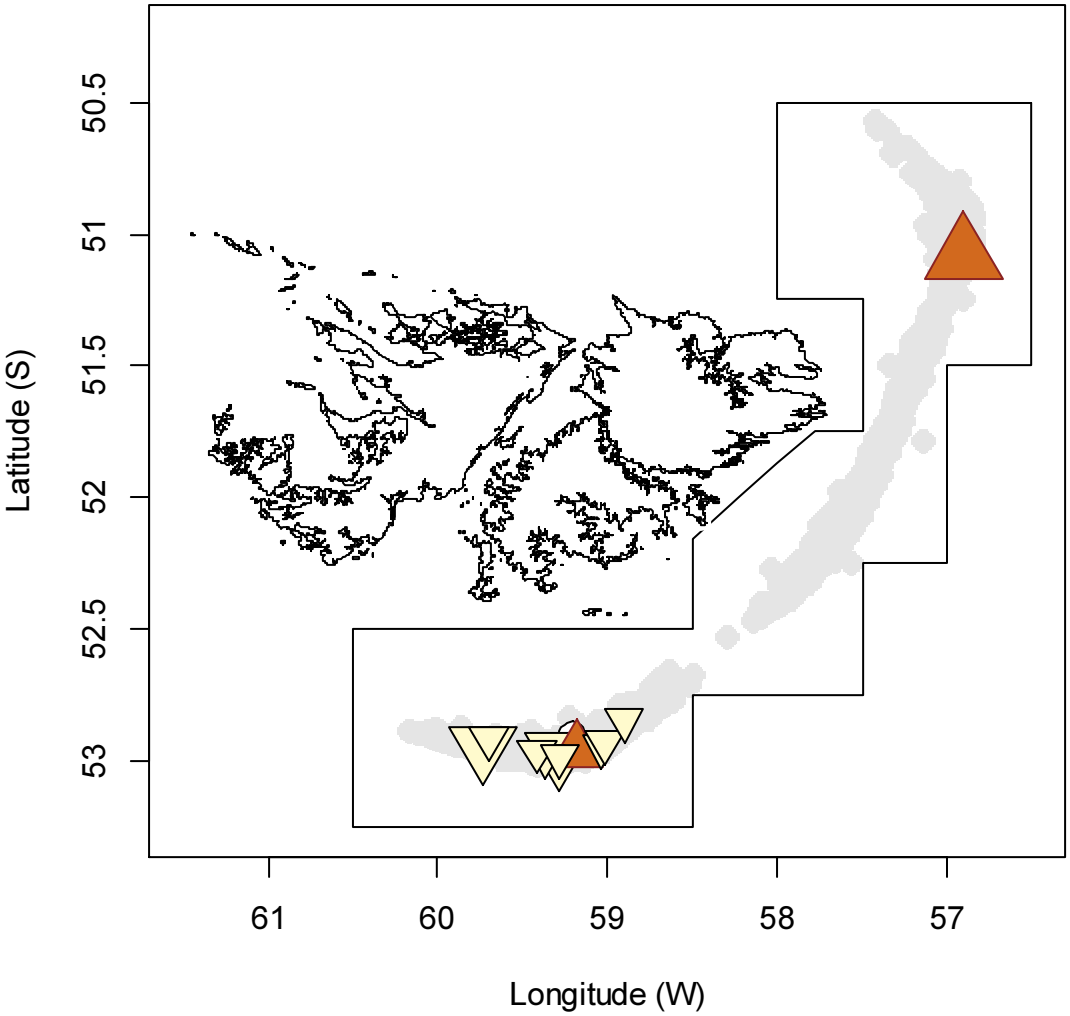

Figure 11. Distribution of pinniped trawl mortalities during the 2nd season. South American fur seals: off-white, point-down. Southern sea lions: brown, point-up. Symbol sizes proportional to square root of mortality numbers. Grey under-shading: distribution of trawls, equivalent to Figure 2.

As a baseline for mortalities, numbers of pinnipeds sighted by observers were examined per trawl per day. 1664 of the 3263 commercial trawls were reported sighted at haul. To examine time series trends, sighting numbers were standardized with GAM for differences in vessels, trawl times and positions. As large proportions of the sightings were zero (809 of 1664 for South American fur seals; 915 of 1664 for Southern sea lions), a delta approach (Pennington 1983, Maunder and Punt 2004) was used to separately model and standardize positive (non-zero) pinniped numbers and the probability of occurrence (presence/absence) of positive numbers, then multiply positive × presence/absence. The standardized sighting numbers were plotted against fishing day and LOESS smooths calculated for the time series trends.

Results of the mortality analysis are summarized in Table 3. Pinniped mortalities were very highly aggregated with all 13 South American fur seals reported killed in only 9 of the 3263 commercial trawls (by 5 of the 17 vessels), and all 6 Southern sea lions reported killed in only 2 of the 3263 commercial trawls (by 2 of the 17 vessels). 2876 of the 3263 commercial trawls were taken after SEDs were mandated on August 5th and August 7th. Correspondingly 9 of 13 South American fur seal mortalities occurred in SED trawls, a proportion that failed to indicate improvement with the use of SEDs. Only 2 of 6 Southern sea lion mortalities occurred in SED trawls, a proportion that did indicate significant improvement with the use of SEDs. This significance is potentially biased because SED implementation was triggered by the precedence of mortalities, rather than assigned a priori, and confounded with chronological progression, as SEDs remained continually in use once they started to be used. However, time series of standardized sighting numbers (Figure 12) suggest that the presence of South American fur seals did not start to significantly change (decrease) in the fishery until around day 251 (September 8th), and the presence of Southern sea lions did not start to significantly change (increase) in the fishery until around day 257 (September 14th); both of which came long after the implementation of SEDs. It may be concluded that under these generally low levels of mortality (e.g., compared to 2017 2nd season, when 57 South American fur seals and 2 Southern sea lions had been killed through August 6th) the effectiveness of SEDs is not easily demonstrated.

Table 3. Hypotheses correlating pinniped mortalities in the 2nd season 2018 commercial fishery. Outcomes are either the mortality counts or the mortality-weighted means of that hypothesis parameter. Non-significant parameters are shaded grey.

Mortality hypothesis	South American fur seal		Southern sea lion	
	Outcome	p	Outcome	p
Without SED	4 / 13	<0.0600	4 / 6	<0.0030
Trawl aggregation[a]	9 / 3263	<0.0001	2 / 3263	<0.0001
Vessel aggregation[b]	5 / 17	<0.0010	2 / 17	<0.0005
Daylight	4 / 13	>0.1000	4 / 6	>0.0750
Lat / Lon position	52.96ºS × 59.37ºW	<0.0001	51.71ºS × 57.67ºW	>0.1000
Trawl duration	5.36 hours	>0.1000	4.50 hours	>0.1000
Sea state[c]	4.15	<0.0300	3.00	>0.1000
Both species				
Non-overlap	0 / 19	>0.9000	-	-

[a] See Table 2.
[b] Vessels not identified, for confidentiality.
[c] Beaufort wind force scale.

In relation to other parameters, South American fur seal mortalities were clearly (Figure 11) and significantly (Table 3) concentrated in the south-west of the Loligo Box. Southern sea lion mortalities occurred in one trawl north-east and one trawl south-west (Figure 11); thus were not significantly correlated with position (Table 3). The parameters of daylight and trawl duration showed no significant correlation with either pinniped species mortality. South American fur seal mortalities occurred in heavier seas than average (Beaufort scale 4.15 vs. 3.35 average), but sea state was not significant according to the adjusted p value = 0.0102 (Equation **13**). The absence of overlap between South American fur seal and Southern sea lion mortalities (Table 2) was entirely non-significant, as given the relative scarcity of mortalities, >90% of randomizations showed no overlap either (Table 3).

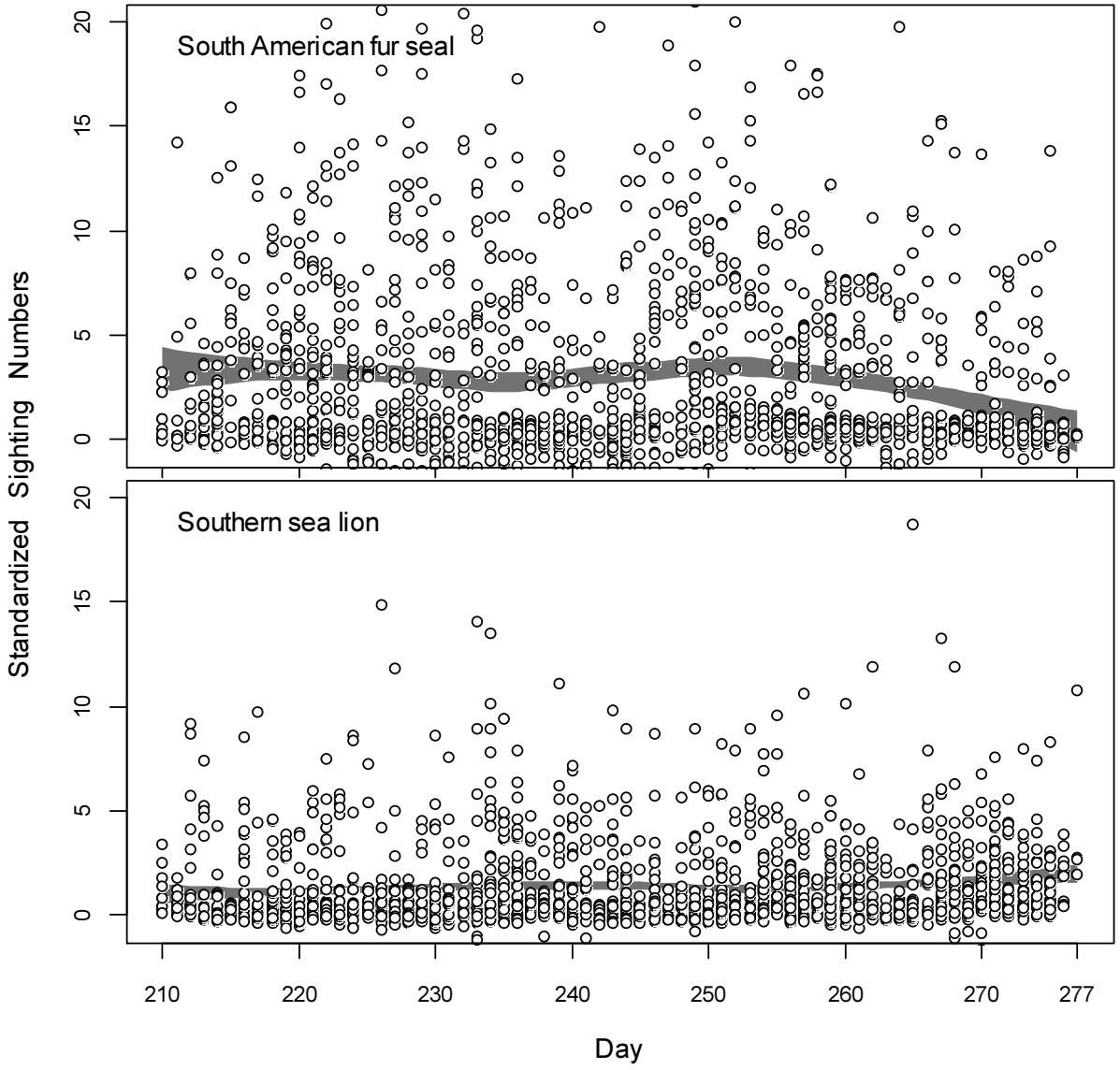

Figure 12. Standardized observer pinniped sighting numbers per trawl by day (n = 1664). Plots are censored for visibility to a max. of 20 sightings; 19 South American fur seal numbers and 1 Southern sea lion number were >20. Note that as an artefact of standardization, some numbers show <0. These negative numbers were not adjusted, in order to maintain consistency of the relative trends over the season (day 210 to day 277). Grey bands on the plots: 95% confidence intervals of LOESS smooths.

Fishery bycatch

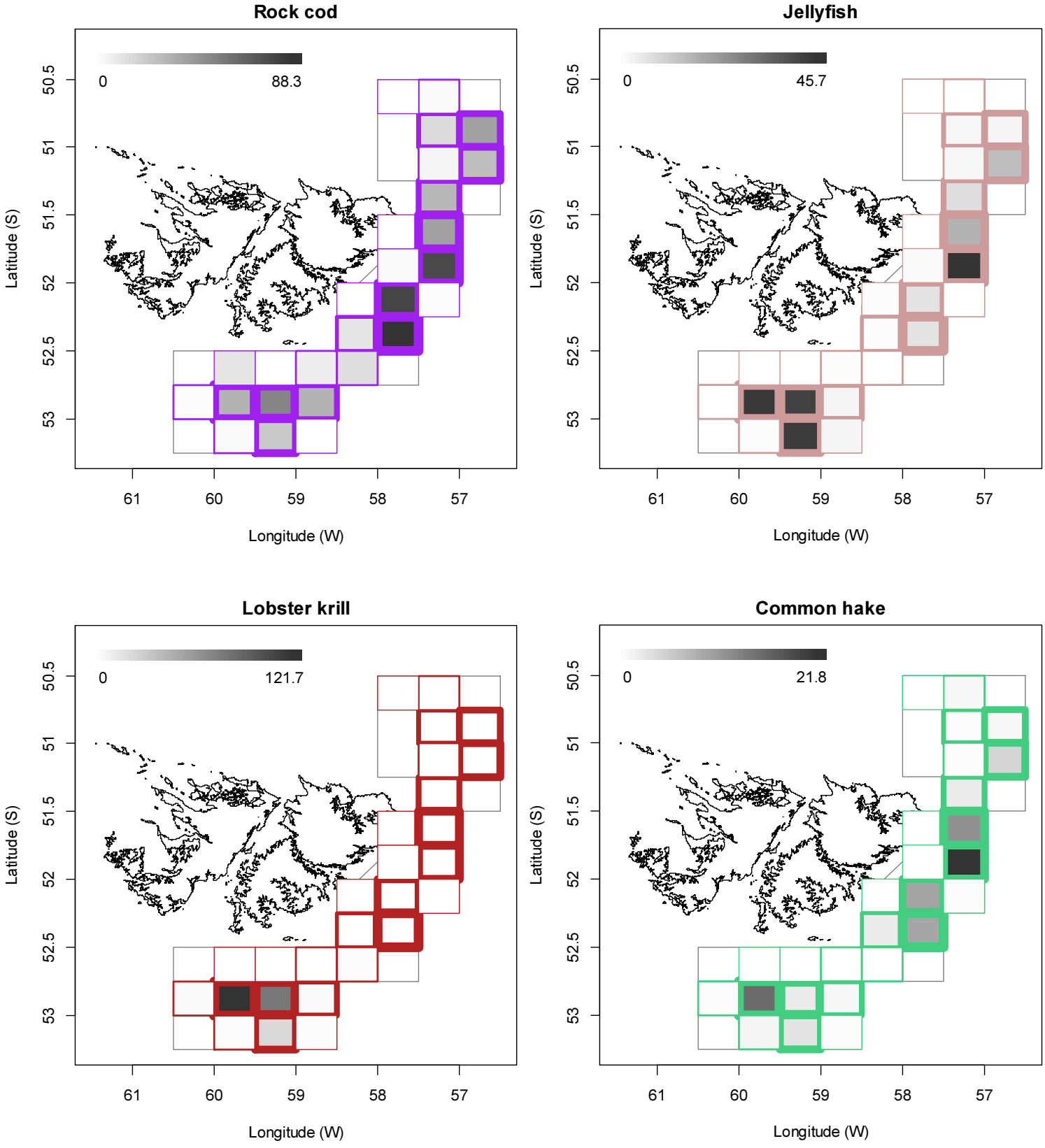

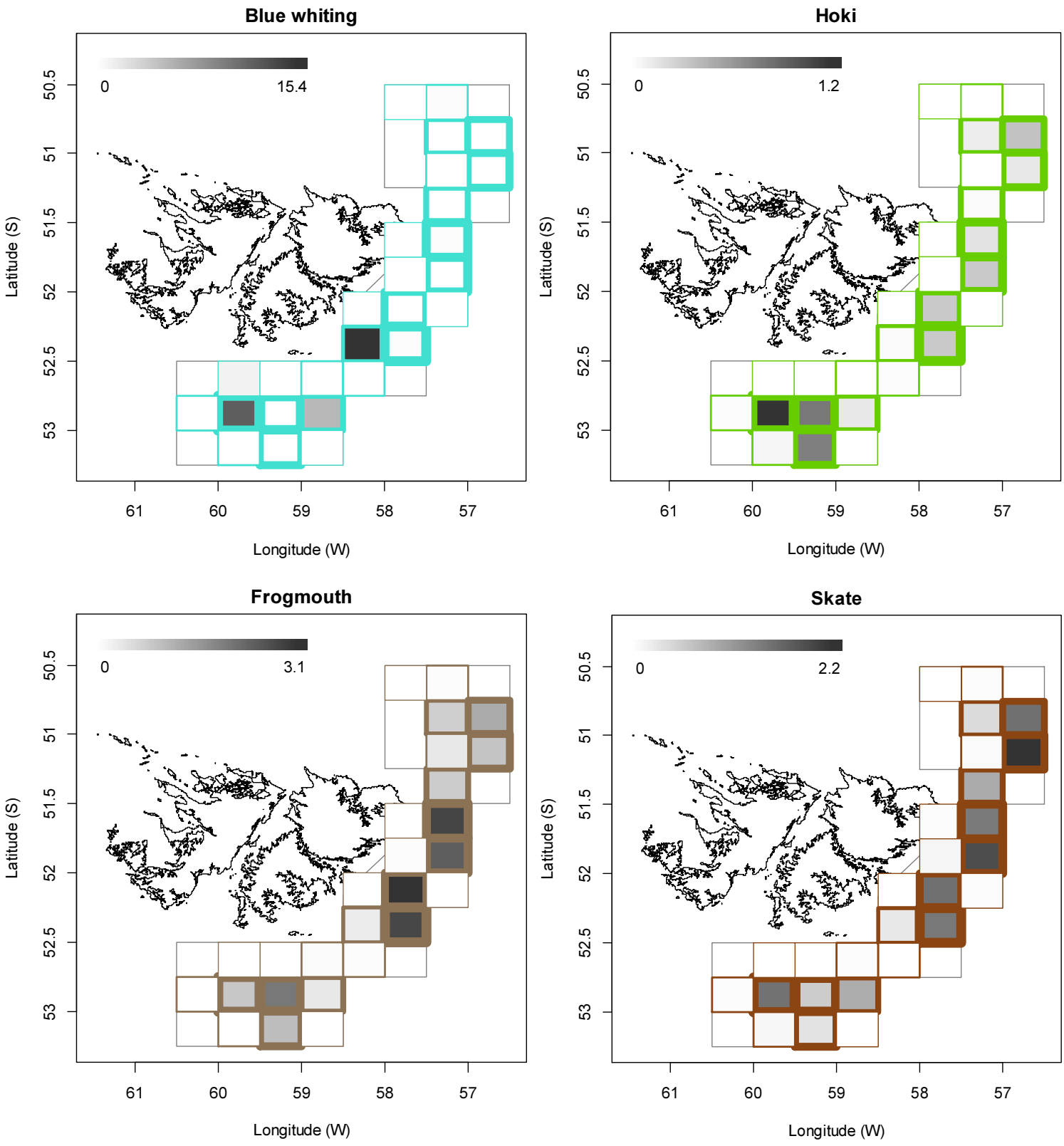

Figure 13. Distributions of the eight principal bycatches during 2nd season 2018, by noon position grids. Thickness of grid lines is proportional to the number of vessel-days (1 to 124 per grid; 27 different grids were occupied). Grey-scale is proportional to the bycatch biomass; maximum (tonnes) indicated on each plot.

Of the 977 2nd season vessel-days (Table 1), 2 vessel-days reported a primary catch of hoki (*Macruronus magellanicus*) rather than *D. gahi* squid, both in the same grid XVAL, by the same vessel, five days apart. One vessel-day (by a different vessel) reported a primary catch of blue whiting (*Micromesistius australis*) rather than *D. gahi*. Hoki and blue whiting catches totalled respectively 26 t from 99 vessel-days, and 35 t from 48 vessel-days. Neither jellyfish (Meduase) nor lobster krill (*Munida* sp.) were primary catches in any vessel-day, but both had the highest 2nd-season totals since at least 2000. As in last season (Winter 2018), jellyfish appeared to be associated with the weather: 31.4% of jellyfish bycatch was taken within 24 hours of one of the three bad-weather days described in Figure 1; the same time span represented 11.6% of season fishing effort. Other high bycatches in 2nd season 2018 were rock cod (*Patagonotothen ramsayi*), as usual, with 605 t from 914 vessel-days, common hake *Merluccius hubbsi* (88 t, 524 vessel-days), frogmouth *Cottoperca gobio* (20 t, 478 vessel-days), and skates Rajiformes (15 t, 418 vessel-days). Relative distributions by grid of these bycatches are shown in Figure 13, and the complete list of all catches by species is given in Table A1.

Seabird bycatch

Thirty-six mortalities of sooty shearwater (*Puffinus griseus*) were recorded in the final week of the season; 33 males and 3 females. All of these mortalities were on the net, not warps. As far as detailed in observer reports, the majority occurred during shooting as the sooty shearwaters tried to scavenge remaining fish scraps (A. Kuepfer, FIFD, personal communication). Other reported bird bycatches throughout the season were four black-browed albatross (*Thalassarche melanophrys*), one Gentoo penguin (*Pygoscelis papua*), and four 'unknown'.

References

Agnew, D.J., Baranowski, R., Beddington, J.R., des Clers, S., Nolan, C.P. 1998. Approaches to assessing stocks of *Loligo gahi* around the Falkland Islands. Fisheries Research 35: 155-169.

Agnew, D. J., Beddington, J. R., and Hill, S. 2002. The potential use of environmental information to manage squid stocks. Canadian Journal of Fisheries and Aquatic Sciences, 59: 1851–1857.

Arkhipkin, A. 1993. Statolith microstructure and maximum age of *Loligo gahi* (Myopsida: Loliginidae) on the Patagonian Shelf. Journal of the Marine Biological Association of the UK 73: 979-982.

Arkhipkin, A.I., Middleton, D.A.J. 2002. Sexual segregation in ontogenetic migrations by the squid *Loligo gahi* around the Falkland Islands. Bulletin of Marine Science 71: 109-127.

Arkhipkin, A.I., Middleton, D.A.J., Barton, J. 2008. Management and conservation of a short-lived fishery resource: *Loligo gahi* around the Falkland Islands. American Fisheries Society Symposium 49: 1243-1252.

Barton, J. 2002. Fisheries and fisheries management in Falkland Islands Conservation Zones. Aquatic Conservation: Marine and Freshwater Ecosystems 12: 127–135.

Brooks, S.P., Gelman, A. 1998. General methods for monitoring convergence of iterative simulations. Journal of computational and graphical statistics 7:434-455.

Chemshirova, I. 2018a. Observer Report 1206. Technical Document, FIG Fisheries Department. 25 p.

Chemshirova, I. 2018b. Observer Report 1209. Technical Document, FIG Fisheries Department. 26 p.

Chen, X., Chen, Y., Tian, S., Liu, B., Qian, W. 2008. An assessment of the west winter-spring cohort of neon flying squid (*Ommastrephes bartramii*) in the Northwest Pacific Ocean. Fisheries Research 92: 221-230.

DeLury, D.B. 1947. On the estimation of biological populations. Biometrics 3: 145-167.

Gamerman, D., Lopes, H.F. 2006. Markov Chain Monte Carlo. Stochastic simulation for Bayesian inference. 2nd edition. Chapman & Hall/CRC.

Hoenig, J.M. 1983. Empirical use of longevity data to estimate mortality rates. Fishery Bulletin 82: 898-903.

Keller, S., Robin, J.P., Valls, M., Gras, M., Cabanellas-Reboredo, M., Quetglas, A. 2015. The use of depletion models to assess Mediterranean cephalopod stocks under the current EU data collection framework. Mediterranean Marine Science 16: 513-523.

Magnusson, A., Punt, A., Hilborn, R. 2013. Measuring uncertainty in fisheries stock assessment: the delta method, bootstrap, and MCMC. Fish and Fisheries 14: 325-342.

Maunder, M.N., Punt, A.E. 2004. Standardizing catch and effort data: a review of recent approaches. Fisheries Research 70: 141-159.

Medellín-Ortiz, A., Cadena-Cárdenas, L., Santana-Morales, O. 2016. Environmental effects on the jumbo squid fishery along Baja California's west coast. Fisheries Science 82: 851-861.

Morales-Bojórquez, E., Hernández-Herrera, A., Cisneros-Mata, M.A., Nevárez-Martínez, M.O. 2008. Improving estimates of recruitment and catchability of jumbo squid *Dosidicus gigas* in the Gulf of California, Mexico. Journal of Shellfish Research 27: 1233-1237.

Nash, J.C., Varadhan, R. 2011. optimx: A replacement and extension of the optim() function. R package version 2011-2.27. http://CRAN.R-project.org/package=optimx

Patterson, K.R. 1988. Life history of Patagonian squid *Loligo gahi* and growth parameter estimates using least-squares fits to linear and von Bertalanffy models. Marine Ecology Progress Series 47: 65-74.

Payá, I. 2010. Fishery Report. *Loligo gahi*, Second Season 2009. Fishery statistics, biological trends, stock assessment and risk analysis. Technical Document, Falkland Islands Fisheries Dept. 54 p.

Pennington, M. 1983. Efficient estimators of abundance, for fish and plankton surveys. Biometrics 39: 281-286.

Pierce, G.J., Guerra, A. 1994. Stock assessment methods used for cephalopod fisheries. Fisheries Research 21: 255 – 285.

Punt, A.E., Hilborn, R. 1997. Fisheries stock assessment and decision analysis: the Bayesian approach. Reviews in Fish Biology and Fisheries 7:35-63.

Roa-Ureta, R. 2012. Modelling in-season pulses of recruitment and hyperstability-hyperdepletion in the *Loligo gahi* fishery around the Falkland Islands with generalized depletion models. ICES Journal of Marine Science 69: 1403–1415.

Roa-Ureta, R., Arkhipkin, A.I. 2007. Short-term stock assessment of *Loligo gahi* at the Falkland Islands: sequential use of stochastic biomass projection and stock depletion models. ICES Journal of Marine Science 64: 3-17.

Rosenberg, A.A., Kirkwood, G.P., Crombie, J.A., Beddington, J.R. 1990. The assessment of stocks of annual squid species. Fisheries Research 8: 335-350.

Royer, J., Périès, P., Robin, J.P. 2002. Stock assessments of English Channel loliginid squids: updated depletion methods and new analytical methods. ICES Journal of Marine Science 59: 445-457.

Shaw, P.W., Arkhipkin, A.I., Adcock, G.J., Burnett, W.J., Carvalho, G.R., Scherbich, J.N., Villegas, P.A. 2004. DNA markers indicate that distinct spawning cohorts and aggregations of Patagonian squid, *Loligo gahi*, do not represent genetically discrete subpopulations. Marine Biology, 144: 961-970.

Swartzman, G., Huang, C., Kaluzny, S. 1992. Spatial analysis of Bering Sea groundfish survey data using generalized additive models. Canadian Journal of Fisheries and Aquatic Sciences 49: 1366-1378.

Thomas, O. 2018. Observer Report 1205. Technical Document, FIG Fisheries Department. 19 p.

Trevizan, T. 2018. Observer Report 1208. Technical Document, FIG Fisheries Department. 24 p.

Winter, A. 2017a. Stock assessment – Falkland calamari (*Doryteuthis gahi*). Technical Document, Falkland Islands Fisheries Department. 30 p.

Winter, A. 2017b. Stock assessment – *Doryteuthis gahi* 2nd season 2017. Technical Document, Falkland Islands Fisheries Department. 37 p.

Winter, A. 2018. Stock assessment – *Doryteuthis gahi* 1st season 2018. Technical Document, Falkland Islands Fisheries Department. 36 p.

Winter, A., Arkhipkin, A. 2015. Environmental impacts on recruitment migrations of Patagonian longfin squid (*Doryteuthis gahi*) in the Falkland Islands with reference to stock assessment. Fisheries Research 172: 85-95.

Winter, A., Zawadowski, T. Thomas, O. 2018. *Doryteuthis gahi* stock assessment survey, 2nd season 2018. Technical Document, Falkland Islands Fisheries Department. 19 p.

Young, I.A.G., Pierce, G.J., Daly, H.I., Santos, M.B., Key, L.N., Bailey, N., Robin, J.-P., Bishop, A.J., Stowasser, G., Nyegaard, M., Cho, S.K., Rasero, M., Pereira, J.M.F. 2004. Application of depletion methods to estimate stock size in the squid *Loligo forbesi* in Scottish waters (UK). Fisheries Research 69: 211-227.

Zhang, H.-M., Bates, J.J., Reynolds, R.W. 2006. Assessment of composite global sampling: Sea surface wind speed. Geophysical Research Letters 33: L17714.

Appendix
***Doryteuthis gahi* individual weights**

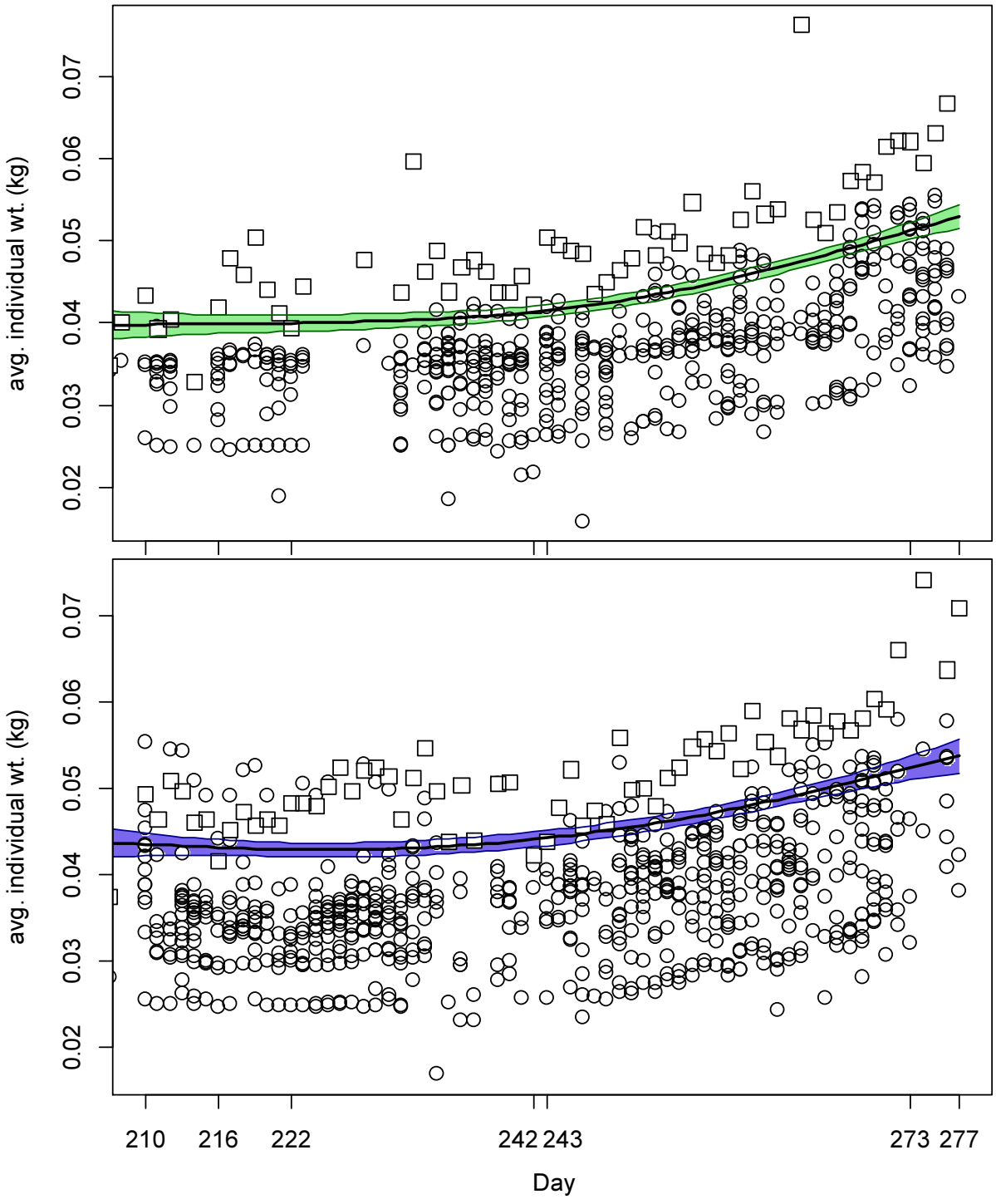

Figure A1. North (top) and south (bottom) sub-area daily average individual *D. gahi* weights from commercial size categories per vessel (circles) and observer measurements (squares). GAMs of the daily trends ± 95% confidence intervals (centre lines and colour under-shading).

To smooth fluctuations, GAM trends were calculated of daily average individual weights. North and south sub-areas were calculated separately. For continuity, GAMs were calculated

using all pre-season survey and in-season data contiguously. North and south GAMs were first calculated separately on the commercial and observer data. Commercial data GAMs were taken as the baseline trends, and calibrated to observer data GAMs in proportion to the correlation between commercial data and observer data GAMs. For example, if the season average individual weight estimate from commercial data was 0.052 kg, the season average individual weight estimate from observer data was 0.060 kg, and the coefficient of determination (R^2) between commercial and observer GAM trends was 86%, then the resulting trend of daily average individual weights was calculated as the commercial data GAM values + (0.060 – 0.052) × 0.86. This way, both the greater day-to-day consistency of the commercial data trends, and the greater point value accuracy of the observer data are represented in the calculations. GAM plots of the north and south sub-areas are shown in Figure A1.

Prior estimates and CV

The pre-season survey (Winter et al. 2018) had estimated *D. gahi* biomasses of 61,262 t north of 52º S and 122,331 t south of 52º S. Hierarchical bootstrapping of the inverse distance weighting algorithm obtained a coefficient of variation (CV) of 0.203 of the biomass distributions. From modelled survey catchability, Payá (2010) had estimated average net escapement of up to 22%, which was added to the CV:

$$61{,}262 \pm (.203 + .22) = 61{,}262 \pm 42.3\% = 61{,}262 \pm 25{,}908 \text{ t} \quad \textbf{(A1-N)}$$

$$122{,}331 \pm (.203 + .22) = 122{,}331 \pm 42.3\% = 122{,}331 \pm 51{,}735 \text{ t} \quad \textbf{(A1-S)}$$

The 22% escapement was added as a linear increase in the variability, but was not used to reduce the total estimate, because squid that escape one trawl are likely to be part of the biomass concentration that is available to the next trawl.

D. gahi numbers at the end of the survey were estimated as survey biomasses divided by the GAM-predicted individual weight averages for the survey: 0.0397 kg north, 0.0438 kg south (Figure A1), and 0.0426 kg combined. Average coefficients of variation (CV) of the GAM over the duration of the pre-season survey were 3.1% north and 2.4% south. CV of the length-weight conversion relationship (Equation **8**) were 8.1% north and 7.8% south. Joining these sources of variation with the pre-season survey biomass estimates and individual weight averages (above) gave estimated *D. gahi* numbers at survey end (day 208) of:

$$_{\text{prior}}N_{\text{N day 208}} = \frac{61{,}262 \times 1000}{0.0397} \pm \sqrt{42.3\%^2 + 3.1\%^2 + 8.1\%^2}$$

$$= 1.544 \times 10^9 \pm 43.2\%$$

$$_{\text{prior}}N_{\text{S day 208}} = \frac{122{,}331 \times 1000}{0.0438} \pm \sqrt{42.3\%^2 + 2.4\%^2 + 7.8\%^2}$$

$$= 2.791 \times 10^9 \pm 43.1\%$$

North and south priors were normalized for the combined fishing zone average, to produce better continuity as vessels cross back and forth between north and south:

$$ {}_{\text{nprior}}N_{\text{N day 208}} = \left(\frac{(61{,}262 + 122{,}331) \times 1000}{0.0426}\right) \times \left(\frac{{}_{\text{prior}}N_{\text{N day 208}}}{{}_{\text{prior}}N_{\text{N day 208}} + {}_{\text{prior}}N_{\text{S day 208}}}\right) $$

$$ = 1.537 \times 10^{9} \pm 43.2\% \qquad \textbf{(A2-N)} $$

$$ {}_{\text{nprior}}N_{\text{S day 208}} = \left(\frac{(122{,}331 + 61{,}262) \times 1000}{0.0426}\right) \times \left(\frac{{}_{\text{prior}}N_{\text{S day 208}}}{{}_{\text{prior}}N_{\text{N day 208}} + {}_{\text{prior}}N_{\text{S day 208}}}\right) $$

$$ = 2.778 \times 10^{9} \pm 43.1\% \qquad \textbf{(A2-S)} $$

The catchability coefficient (q) prior for the north sub-area was calculated on day 210, when three vessels first fished north and the initial depletion period north started. Abundance on day 210 was discounted for natural mortality over the 2 days since the end of the survey:

$$ {}_{\text{nprior}}N_{\text{N day 210}} = {}_{\text{nprior}}N_{\text{N day 210}} \times e^{-M \cdot (210 - 208)} - \text{CNMD}_{\text{N day 210}} = 1.496 \times 10^{9} \qquad \textbf{(A3-N)} $$

where $\text{CNMD}_{\text{N day 58}} = 0$ as no catches had been taken between day 56 and day 58. Thus:

$$ {}_{\text{prior}}q_{\text{N}} = C(N)_{\text{N day 210}} / ({}_{\text{nprior}}N_{\text{N day 210}} \times E_{\text{N day 210}}) $$

$$ = (C(B)_{\text{N day 210}} / \text{Wt}_{\text{N day 210}}) / ({}_{\text{nprior}}N_{\text{N day 210}} \times E_{\text{N day 210}}) $$

$$ = (236.6 \text{ t} / 0.0398 \text{ kg}) / (1.496 \times 10^{9} \times 3 \text{ vessel-days}) $$

$$ = 1.325 \times 10^{-3} \text{ vessels}^{-1} \text{ [f]} \qquad \textbf{(A4-N)} $$

CV of the prior was calculated as the sum of variability in ${}_{\text{nprior}}N_{\text{S day 208}}$ (Equations **A2-N**) plus variability in the catches of vessels on start day 210, plus variability of the natural mortality (see Appendix section Natural mortality, below):

$$ CV_{\text{prior N}} = $$

$$ \sqrt{43.2\%^2 + \left(\frac{\text{SD}\left(C(B)_{\text{N vessels day 210}}\right)}{\text{mean}\left(C(B)_{\text{N vessels day 210}}\right)}\right)^2 + (1 - \text{sign}(1 - CV_M) \times \text{abs}(1 - CV_M)^{(210-208)})^2} $$

$$ = \sqrt{43.2\%^2 + 29.1\%^2 + 28.5\%^2} = 59.4\% \qquad \textbf{(A5-N)} $$

The catchability coefficient (q) prior for the south sub-area was taken on day 210, the first day of the season, when 13 vessels fished in the south and the initial depletion period south started. Abundance on day 210 was discounted for natural mortality over the 2 days since the end of the survey:

$$ {}_{\text{nprior}}N_{\text{S day 210}} = {}_{\text{nprior}}N_{\text{S day 208}} \times e^{-M \cdot (210 - 208)} - \text{CNMD}_{\text{S day 210}} = 2.705 \times 10^{9} \qquad \textbf{(A3-S)} $$

where $\text{CNMD}_{\text{S day 58}} = 0$ as no catches intervened between the end of the survey and the start of commercial season. Thus:

[f] On Figure 6-left.

$$_{\text{prior}}q_{S} = C(N)_{S\ \text{day}\ 210} / ({}_{\text{nprior}}N_{S\ \text{day}\ 210} \times E_{S\ \text{day}\ 210})$$

$$= (C(B)_{S\ \text{day}\ 210} / Wt_{S\ \text{day}\ 210}) / ({}_{\text{nprior}}N_{S\ \text{day}\ 210} \times E_{S\ \text{day}\ 210})$$

$$= (761.3\ \text{t} / 0.0435\ \text{kg}) / (2.705 \times 10^{9} \times 13\ \text{vessel-days})$$

$$= 0.498 \times 10^{-3}\ \text{vessels}^{-1}\ ^{g} \qquad \textbf{(A4-S)}$$

CV of the prior was calculated as the sum of variability in $_{\text{nprior}}N_{S\ \text{day}\ 208}$ (Equations **A2-S**) plus variability in the catches of vessels on start day 210, plus variability of the natural mortality (see Appendix section Natural mortality, below):

$$CV_{\text{prior S}} =$$

$$\sqrt{43.1\%^2 + \left(\frac{\text{SD}\left(C(B)_{S\ \text{vessels day}\ 210}\right)}{\text{mean}\left(C(B)_{S\ \text{vessels day}\ 210}\right)}\right)^2 + (1 - \text{sign}(1 - CV_M) \times \text{abs}(1 - CV_M)^{(210-208)})^2}$$

$$= \sqrt{43.1\%^2 + 20.4\%^2 + 28.5\%^2} \quad = 55.5\% \qquad \textbf{(A5-S)}$$

Depletion model estimates and CV

For the north sub-area, the equivalent of Equation **3** with three N_{day} was optimized on the difference between predicted catches and actual catches (Equation **4**), resulting in parameters values:

$$_{\text{depletion}}N1_{N\ \text{day}\ 210} = 0.518 \times 10^{9}; \quad {}_{\text{depletion}}N2_{N\ \text{day}\ 243} = 4$$

$$_{\text{depletion}}N3_{N\ \text{day}\ 273} = 0$$

$$_{\text{depletion}}q_{N\ \text{NSED}} = 2.741 \times 10^{-3}\ ^{h}$$

$$_{\text{depletion}}q_{N\ \text{SED}} = 3.642 \times 10^{-3} \qquad \textbf{(A6-N)}$$

The root-mean-square deviation of predicted vs. actual catches was calculated as the CV of the model:

$$CV_{\text{rmsd N}} = \frac{\sqrt{\sum_{i=1}^{n}\left({}_{\text{predicted}}C(N)_{N\ \text{day}\ i} - {}_{\text{actual}}C(N)_{N\ \text{day}\ i}\right)^2 / n}}{\text{mean}\left({}_{\text{actual}}C(N)_{N\ \text{day}\ i}\right)}$$

$$= 1.340 \times 10^{6} / 4.232 \times 10^{6} = 31.7\% \qquad \textbf{(A7-N)}$$

$CV_{\text{rmsd N}}$ was added to the variability of the GAM-predicted individual weight averages for the season (Figure A1-N); equal to a CV of 1.7% north. CVs of the depletion were then calculated as the sum:

[g] On Figure 8-left.
[h] On Figure 6-left.

$$CV_{\text{depletion N}} = \sqrt{CV_{\text{rmsd N}}^{\,2} + CV_{\text{GAM Wt N}}^{\,2}} = \sqrt{31.7\%^2 + 1.2\%^2}$$

$$= 31.7\% \qquad \textbf{(A8-N)}$$

For the south sub-area, the equivalent of Equation **3** with four N_{day} was optimized on the difference between predicted catches and actual catches (Equation **4**), resulting in parameters values:

$$_{\text{depletion}}N1_{\text{S day 210}} = 0.976 \times 10^{9}; \quad _{\text{depletion}}N2_{\text{S day 216}} = 0$$
$$_{\text{depletion}}N3_{\text{S day 222}} = 3627; \quad _{\text{depletion}}N4_{\text{S day 242}} = 0$$
$$_{\text{depletion}}q_{\text{S NSED}} = 1.681 \times 10^{-3}\ ^{i}$$
$$_{\text{depletion}}q_{\text{S SED}} = 2.216 \times 10^{-3} \qquad \textbf{(A6-S)}$$

The normalized root-mean-square deviation of predicted vs. actual catches was calculated as the CV of the model:

$$CV_{\text{rmsd S}} = \frac{\sqrt{\sum_{i=1}^{n}\left({}_{\text{predicted}}C(N)_{\text{S day i}} - {}_{\text{actual}}C(N)_{\text{S day i}}\right)^2 / n}}{\text{mean}\left({}_{\text{actual}}C(N)_{\text{S day i}}\right)}$$

$$= 3.953 \times 10^{6} / 7.352 \times 10^{6} = 53.8\% \qquad \textbf{(A7-S)}$$

$CV_{\text{rmsd S}}$ was added to the variability of the GAM-predicted individual weight averages for the season (Figure A1-S); equal to a CV of 1.05% south. CVs of the depletion were then calculated as the sum:

$$CV_{\text{depletion S}} = \sqrt{CV_{\text{rmsd S}}^{\,2} + CV_{\text{GAM Wt S}}^{\,2}} = \sqrt{53.8\%^2 + 1.05\%^2}$$

$$= 53.8\% \qquad \textbf{(A8-S)}$$

Combined Bayesian models

For the north sub-area, joint optimization of Equations **4** and **5** resulted in parameters values:

$$_{\text{Bayesian}}N1_{\text{N day 210}} = 0.569 \times 10^{9}; \quad _{\text{Bayesian}}N2_{\text{N day 243}} = 4$$
$$_{\text{Bayesian}}N3_{\text{N day 273}} = 0$$
$$_{\text{Bayesian}}q_{\text{N NSED}} = 1.635 \times 10^{-3}\ ^{j}$$
$$_{\text{Bayesian}}q_{\text{N SED}} = 2.937 \times 10^{-3} \qquad \textbf{(A9-N)}$$

These parameters produced the fit between predicted catches and actual catches shown in Figure A2-N.

Figure A2-N [next page]. Daily catch numbers estimated from actual catch (black points: without SEDs, black triangles: with SEDs) and predicted from the depletion model (green line) in the north sub-area.

[i] On Figure 8-left.
[j] On Figure 6-left.

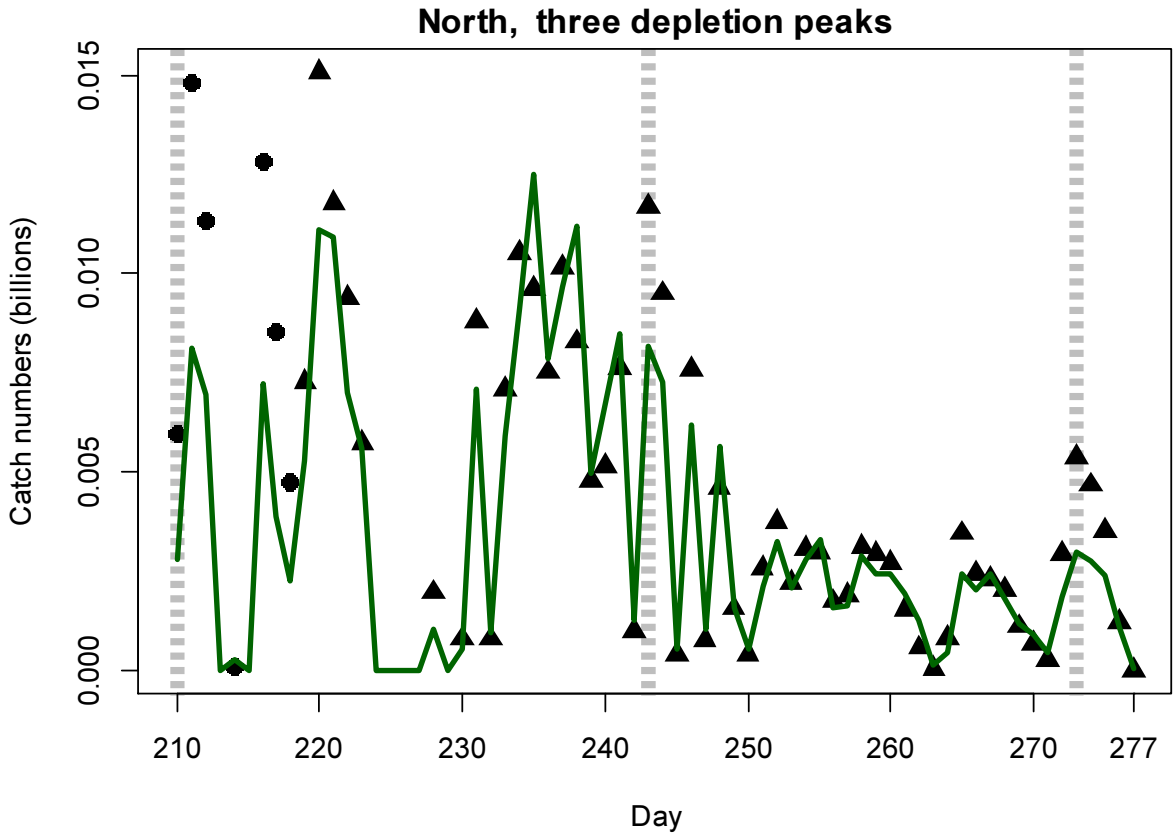
North, three depletion peaks
Catch numbers (billions)
0.000
0.005
0.010
0.015
210
220
230
240
250
260
270
277
Day

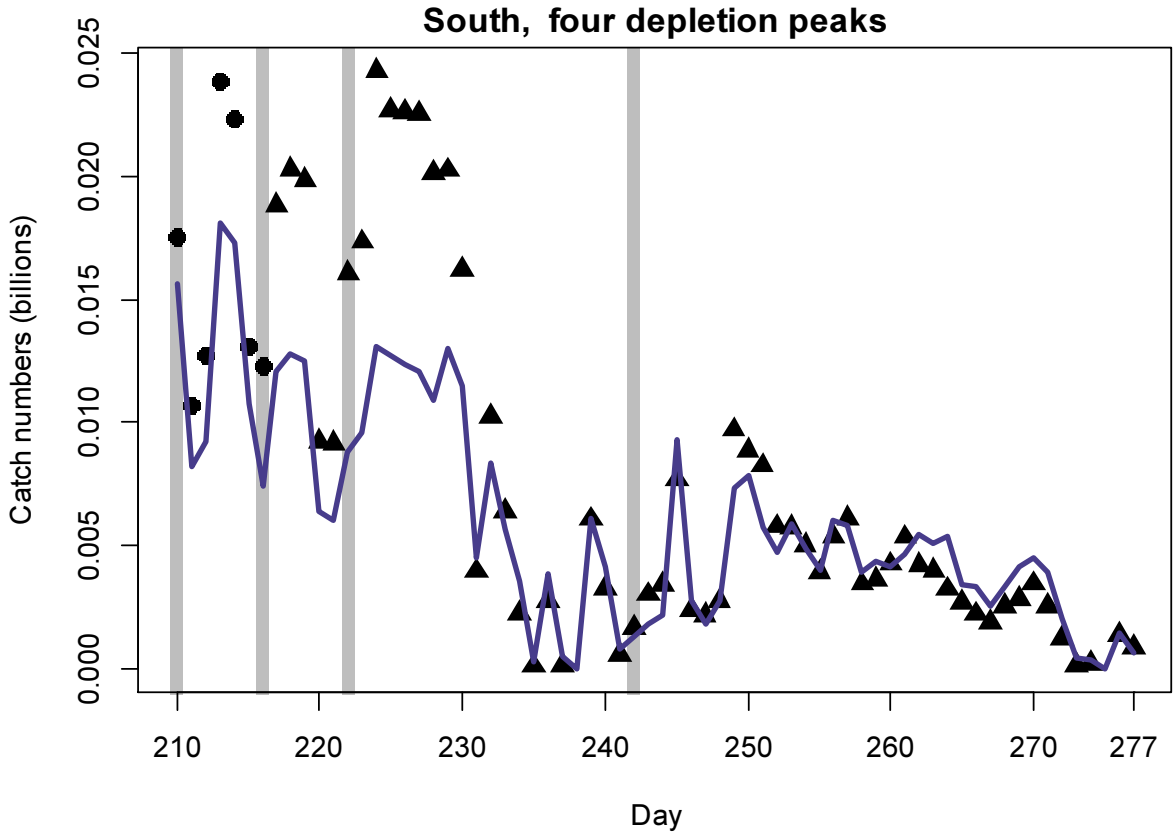
South, four depletion peaks
Catch numbers (billions)
0.000
0.005
0.010
0.015
0.020
0.025
210
220
230
240
250
260
270
277
Day

Figure A2-S [previous page]. Daily catch numbers estimated from actual catch (black points: without SEDs, black triangles: with SEDs) and predicted from the depletion model (purple line) in the south sub-area.

For the south sub-area, the joint optimization of Equations **4** and **5** resulted in parameters values:

$$\begin{aligned} {}_{\text{Bayesian}}N1_{\text{S day 210}} &= 2.220 \times 10^{9}; & {}_{\text{Bayesian}}N2_{\text{S day 216}} &= 16 \\ {}_{\text{Bayesian}}N3_{\text{S day 222}} &= 0; & {}_{\text{Bayesian}}N4_{\text{S day 242}} &= 7 \\ {}_{\text{Bayesian}}q_{\text{S NSED}} &= 0.544 \times 10^{-3} \text{ [k]} \\ {}_{\text{Bayesian}}q_{\text{S SED}} &= 0.575 \times 10^{-3} \end{aligned} \quad \textbf{(A9-S)}$$

These parameters produced the fit between predicted catches and actual catches shown in Figure A2-S.

Natural mortality

Natural mortality is parameterized as a constant instantaneous rate M = 0.0133 day^{-1} (Roa-Ureta and Arkhipkin 2007), based on Hoenig's (1983) log mortality vs. log maximum age regression applied to an estimated maximum age of 352 days for *Doryteuthis gahi*:

$$\begin{aligned} \log(M) &= 1.44 - 0.982 \times \log(\text{age}_{\max}) \\ M &= \exp(1.44 - 0.982 \times \log(352)) \\ &= 0.0133 \end{aligned} \quad \textbf{(A10)}$$

Hoenig (1983) derived Equation **A10** from the regression of 134 stocks among 79 species of fish, molluscs, and cetaceans. Hoenig's regression obtained $R^2 = 0.82$, but a corresponding coefficient of variation (CV) was not published. An approximate CV of M was estimated by measuring the coordinates off a print of Figure 1 in Hoenig (1983) and repeating the regression. Variability of M was calculated by randomly re-sampling, with replacement, the regression coordinates 10000× and re-computing Equation **A10** for each iteration of the resample (Winter 2017a). The CV of M from the 10000 random resamples was:

$$\begin{aligned} CV_M &= SD_M / Mean_M \\ CV_M &= 0.0021 / 0.0134 = 15.46\% \end{aligned} \quad \textbf{(A11)}$$

CV_M over the aggregate number of unassessed days between survey end and commercial season start was then added to the CV of the biomass prior estimate and the CV of variability in vessel catches on start day (**A5-N** and **A5-S**). CV_M was further expressed as an absolute value and indexed by sign(1 - CV_M) to ensure that the value could not decrease if CV_M was hypothetically > 100%.

[k] On Figure 8-left.

Total catch by species

Table A1: Total reported catches and discard by taxon during second season 2018 X-license fishing, and number of catch reports in which each taxon occurred. Does not include incidental catches of pinnipeds or seabirds.

Species Code	Species / Taxon	Catch Wt. (KG)	Discard Wt. (KG)	N Reports
LOL	*Doryteuthis gahi*	35827955	16077	977
PAR	*Patagonotothen ramsayi*	604597	602547	914
MED	Medusae sp.	243364	243364	455
MUN	*Munida* spp.	235116	235116	259
HAK	*Merluccius hubbsi*	87946	8450	524
BLU	*Micromesistius australis*	34969	2484	48
WHI	*Macruronus magellanicus*	26154	2404	99
CGO	*Cottoperca gobio*	19750	19750	478
RAY	Rajiformes	14895	7101	418
BAC	*Salilota australis*	11274	588	92
TOO	*Dissostichus eleginoides*	4560	4111	336
UCH	Sea urchin	4060	4060	42
GRV	*Macrourus* spp.	3665	2650	81
GRC	*Macrourus carinatus*	2160	55	13
DGH	*Schroederichthys bivius*	1458	1458	119
SCA	Scallop	1119	1119	26
KIN	*Genypterus blacodes*	785	536	82
DGS	*Squalus acanthias*	536	536	7
ING	*Moroteuthis ingens*	211	211	44
GRF	*Coelorinchus fasciatus*	170	170	3
PAT	*Merluccius australis*	105	37	7
PTE	*Patagonotothen tessellata*	89	89	6
SPN	Porifera	85	85	3
LAR	*Lampris immaculatus*	75	75	1
OCT	*Octopus* spp.	69	69	6
MUL	*Eleginops maclovinus*	60	60	16
SOM	*Somniosus microcephalus*	57	57	1
OTH	–	53	53	3
ILL	*Illex argentinus*	31	31	3
MYX	*Myxine* spp.	27	27	6
DGX	Dog / Cat shark uid.	10	10	1
RED	*Sebastes oculatus*	8	8	3
COT	*Cottunculus granulosus*	4	4	1
LIM	*Lithodes murrayi*	3	3	1
BDU	*Brama dussumieri*	3	3	2
Total		37125423	1153398	977